U.PORTO

MESTRADO EM ONCOLOGIA

ONCOLOGIA LABORATORIAL

The effect of iron and Nrf2 on endothelial cells - the retinal angiogenesis as a model

Cristina Ramos Abreu

M

2021

Cristina Ramos Abreu. The effect of iron and Nrf2 on endothelial cells - the retinal angiogenesis as a model

M. ICBAS **2021**

U.PORTO

The effect of iron and Nrf2 on endothelial cells - the retinal angiogenesis as a model

Cristina Sofia Ramos Abreu

INSTITUTO DE CIÊNCIAS BIOMÉDICAS ABEL SALAZAR

CRISTINA SOFIA RAMOS ABREU

THE EFFECT OF IRON AND NRF2 ON ENDOTHELIAL CELLS – THE RETINAL ANGIOGENESIS AS A MODEL

Dissertação de Candidatura ao grau de Mestre em Oncologia – Oncologia Laboratorial – submetida ao Instituto de Ciências Biomédicas de Abel Salazar da Universidade do Porto

Orientador – Doutor Delfim Duarte

Categoria – Professor Auxiliar Convidado/Investigador/Médico Interno

Afiliação – IPO-Porto / IBMC-I3S / FMUP

Co-orientador – Doutora Graça Porto

Categoria – Professora Catedrática Convidada

Afiliação – ICBAS-UP

Dedicatória

Dedico esta dissertação aos meus queridos pais,
por todo o apoio incondicional diário ao longo deste percurso e sempre.

Persistir, insistir e nunca desistir.

ACKNOWLEDGEMENTS

Esta dissertação é fruto de um projeto desenvolvido no Mestrado em Oncologia. Contudo, todo o meu conhecimento e trabalho desenvolvido provém de um esforço e longo caminho durante estes últimos anos da minha vida. Várias pessoas deram o seu contributo pessoal e profissional para que esta meta fosse atingida, mas principalmente, as que serão em seguida mencionadas foram, sem dúvida, as mais marcantes e importantes. Assim, é imprescindível agradecer-lhes:

Em primeiro lugar quero agradecer do fundo do coração ao meu orientador Dr. Delfim Duarte por todo o conhecimento transmitido, acompanhamento, disponibilidade, e principalmente, por toda a sua compreensão e paciência. Quero também agradecer à minha co-orientadora Dra. Graça Porto.

Aos meus restantes colegas de trabalho, Marta, Laura, Joana e Tiago que me receberam de braços abertos neste grupo de investigação. Foi um prazer trabalhar convosco.

À minha querida e tão especial amiga Maria que me acompanha nesta longa caminhada desde a licenciatura.

Às minhas colegas de mestrado, Margarida, Telma e Cristina que deixaram de ser meras colegas e se tornaram amigas para a vida toda.

À minha amiga Rita que tive a sorte de um dia a conhecer. Mais que uma amiga, tem sido uma irmã.

Quase finalizando, quero agradecer à minha querida mãe, a mulher que mais me inspira força e dedicação, ao meu pai e ao meu irmão por todo o apoio e amor incondicional.

A minha avó Conceição, que sem dúvida, é a maior estrela que o céu um dia ganhou. Sei que olhas todos os dias por mim.

Por fim, quero agradecer a todos aqueles que direta ou indiretamente contribuíram de alguma forma para que eu conseguisse alcançar este objetivo com sucesso.

Muito obrigada a todos!

TABLE OF CONTENTS

ABSTRACT

Growing evidence supports the involvement of angiogenesis in the pathophysiology of hematologic malignancies. Increased bone marrow microvessel density has been consistently reported in patients with Acute Myeloid Leukemia resulting in a decreased response to induction therapy, and more recent work from our group has shown that by restoring blood vessels in the endosteum, it was possible to increase chemotherapy delivery and protect non-malignant hematopoiesis. Among other factors, iron plays an essential role in tumor progression and metastasis formation playing an active role in the survival of tumor cells and reprogramming of the tumor microenvironment. The role of iron in the process of angiogenesis is still largely unknown.

In order to better understand the biological steps involved in the angiogenesis process it is fundamental to develop an optimal experimental vascular model. The mouse retina offers an excellent model to study angiogenesis *in vivo*. The retina is one of the few places in the body where blood vessels might be directly observed and analyzed in a physiological context. Moreover, retinal development in mice can be accessed postnatally, which is a major advantage for imaging and modeling the developing vasculature without the difficulties associated with investigating embryonic development. Among the pending questions in retinal physiology, the mechanisms how iron in excess causes retinal degeneration and leads to loss of its function is a major asset and needs to be explored. One of the candidate players in this setting is Nrf2, an intracellular transcription factor that regulates the expression of a number of genes to encode anti-oxidative enzymes, anti-apoptotic proteins, detoxifying factors, and drug transporters.

In the experimental work developed in this thesis we used the well-described retinal angiogenesis as a model to study the *in vivo* iron-induced damage of endothelial cells and the putative role of Nrf2 in this process. We analysed the three-dimensional retinal vascular architecture in postnatal day 5 in mice and assessed the anatomical features of the retinal vasculature, the parameters of the developing vasculature network namely the vascular length and vascular outgrowth, the number of arteries and vessels, and the presence of microhemorrhages. Our results show that specific heterozygous Nrf2 knockout (Cdh5-CreER;$Nrf2^{lox/+}$) mice that were generated did not show particular

vascular defects, decreased angiogenesis or increased vascular permeability in response to iron dextran administration. We speculate that the partial expression of Nrf2 in endothelial cells from Cdh5-CreER;$Nrf2^{lox/+}$ may be sufficient to adequately respond to iron toxicity. As a future work we need to analyse Cdh5-CreER;$Nrf2^{lox/lox}$, which have total loss of Nrf2 expression in endothelial cells.

RESUMO

Evidências crescentes apoiam o envolvimento da angiogénese na fisiopatologia das malignidades hematológicas. O aumento da densidade de microvasos da medula óssea foi relatado de forma consistente em pacientes com leucemia mieloide aguda, resultando em uma resposta diminuída à terapia de indução, e um trabalho mais recente do nosso grupo mostrou que, ao restaurar os vasos sanguíneos no endósteo, foi possível aumentar a administração de quimioterapia e proteger a hematopoiese não maligna. Entre outros fatores, o ferro desempenha um papel essencial na progressão tumoral e formação de metástases, desempenhando um papel ativo na sobrevivência das células tumorais e na reprogramação do microambiente tumoral. O papel do ferro no processo de angiogénese ainda é amplamente desconhecido.

Para melhor compreender as etapas biológicas envolvidas no processo de angiogénese, é fundamental desenvolver um modelo vascular experimental ideal. A retina do ratinho oferece um excelente modelo para estudar a angiogénese *in vivo*. A retina é um dos poucos lugares do corpo onde os vasos sanguíneos podem ser diretamente observados e analisados em um contexto fisiológico. Além disso, o desenvolvimento da retina em ratinhos pode ser acessado após o nascimento, o que é uma grande vantagem para a imagem e modelagem da vasculatura em desenvolvimento sem as dificuldades associadas à investigação do desenvolvimento embrionário. Entre as questões pendentes na fisiologia da retina, os mecanismos pelos quais o ferro em excesso causa degeneração da retina e leva à perda de sua função é um ativo importante e precisa ser explorado. Um dos jogadores candidatos neste cenário é o Nrf2, um fator de transcrição intracelular que regula a expressão de vários genes para codificar enzimas antioxidantes, proteínas anti-apoptóticas, fatores de desintoxicação e transportadores de drogas.

No trabalho experimental desenvolvido nesta tese utilizamos a bem descrita angiogénese retinal como modelo para estudar o dano in vivo às células endoteliais induzido por ferro e o suposto papel do Nrf2 neste processo. Analisamos a arquitetura vascular retiniana tridimensional no dia 5 pós-natal em ratinhos e avaliamos as características anatómicas da vasculatura retiniana, os parâmetros da rede de vasculatura em desenvolvimento, nomeadamente o comprimento vascular e o crescimento vascular, o número de artérias e vasos e

a presença de microhemorragias. Nossos resultados mostram que ratinhos nocautes heterozigotos específicos para Nrf2 (Cdh5-CreER; Nrf2lox / +) que foram gerados não apresentaram defeitos vasculares particulares, diminuição da angiogénese ou aumento da permeabilidade vascular em resposta à administração de ferro dextrano. Especulamos que a expressão parcial de Nrf2 em células endoteliais de Cdh5-CreER; $Nrf2^{lox/+}$ pode ser suficiente para responder adequadamente à toxicidade do ferro. Como trabalho futuro, precisamos analisar Cdh5-CreER; $Nrf2^{lox/lox}$, que apresentam perda total da expressão de Nrf2 em células endoteliais.

LIST OF FIGURES

LIST OF TABLES

ABREVIATIONS

AML	Acute Myeloid Leukemia
APL	Acute promyelocytic leukemia
BM	Bone marrow
CR	Complete remission
CDH5	Cadherin 5
DGAV	Direção-Geral de Alimentação e Veterinária
DMSO	Dimethylsulfoxide
EC	Endothelial cells
ER	Estrogen receptor
ER-LBD	Estrogen receptor ligand-binding domain
FBS	Fetal Bovine Serum
FPN	Ferroportin
HmO-1	Heme oxygenase-1
HSCs	Hematopoietic stem cells
HSP90	Heat Shocked Protein
IARC	International Agency for Research on Cancer
MDS	Myelodysplastic syndromes
ML	Myeloid leukemia
MRD	Measurable residual disease
MVD	Microvessel density
Nrf2	Nuclear factor erythroid 2-related factor 2
$O2^{\cdot -}$	Superoxide anion radical
$OH^{\cdot}$	Hydroxyl radical
PB	Peripheral blood
PBS	Phosphate Buffered Saline
PBMCs	Peripheral blood mononuclear cells
PBS-T	Phosphate Buffered Saline Treatment
PFA	Paraformaldehyde
ROS	Oxygen species
RT	Room temperature
SF	Serum ferritin
TSAT	Transferrin saturation
VD	Vascular Density
VL	Vascular Length
VOg	Vascular Outgrowth
VEGF	Vascular Endothelial Growth Factor

WHO	World Health Organization

CHAPTER 1. BACKGROUND

1. Cancer

1.1. Epidemiology

Cancer is a major public health problem worldwide, where millions of people live with a cancer diagnosis[1]. According to the International Agency for Research on Cancer (IARC) of the World Health Organization (WHO), cancer is a chronic disease, responsible for several deaths worldwide, with a higher number of new cases in developed countries compared to developing countries, as depicted in figure 1.

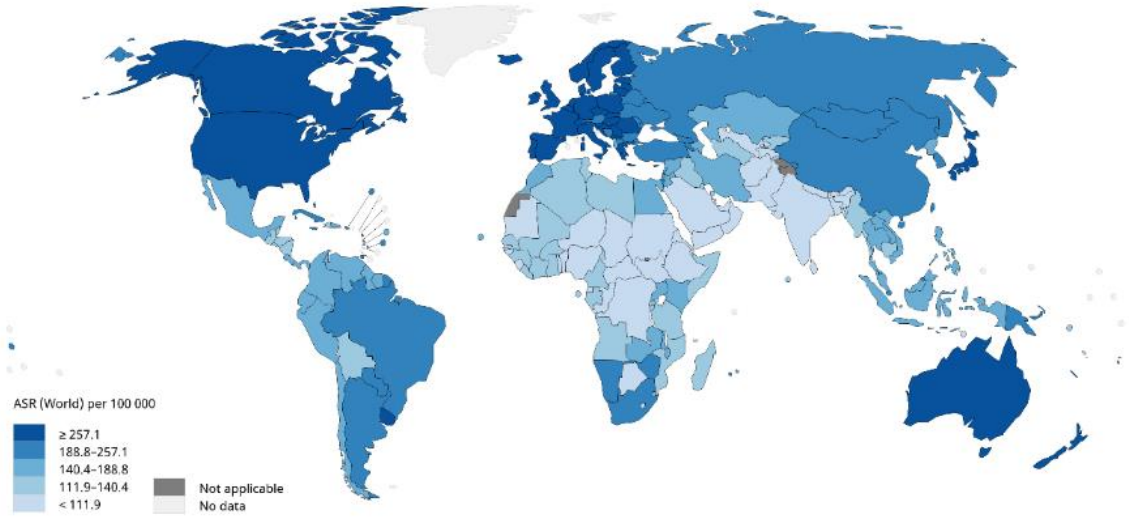

Figure 1 - Estimated number of incidence cases (5 years) as a proportion in 2020, for all cancers, both sexes, all ages (World). Data source: International Agency for Research on Cancer, GLOBOCAN January, 2021.

Over the years there has been constant research to better understand cancer biology, its main causes and develop effective treatments. Despite significant advances in the prevention, detection, and treatment of cancer, there are still many open questions and a need to improve the quality of life and survival of patients.

Leukemia is a cancer of the most primitive cells in the bone marrow (BM) – hematopoietic stem and progenitor cells – which have different levels of self-renewal and multipotency properties and give rise to differentiated blood cells. The BM is where the process of blood production or hematopoiesis takes place[2].

Acute Myeloid Leukemia (AML), a specific subtype of leukemia, is one of the most common types of cancer in adults and its incidence peaks in individuals over 60 years of age (average patient age is around 68 years)[3, 4]. In 2002, AML was responsible for about 30% of all leukaemias in adults, and about 18,300 new cases are diagnosed in Europe each year which represents 0,6% of all cancers[5, 6]. The statistical data point to annual incidence rates in Europe of 2-4 per 100,000 individuals. In Portugal, according to data from National Oncology Registry, 367 new AML cases were diagnosed in 2010. In 2018 the estimated prevalence in Portugal was of 709 patients, with 251 new cases appearing per year and with a higher incidence in patients aged 70-79 years. AML is an aggressive cancer, and its overall five-year survival rate is roughly 25% [7].

1.2. Acute myeloid Leukemia – General characterization

AML is defined as an hematological cancer that occurs as a consequence of genetic alterations in hematopoietic progenitors, leading to a blockage in differentiation and an unbalanced growth of leukemia blasts in the BM[8].

Regarding its morphology, AML blasts could vary in size from slightly larger than lymphocytes to the size of monocytes or larger[9]. The nuclei vary in shape, are large and frequently contain several nucleoli. AML blast express antigens, found also on healthy immature myeloid cells, including the markers CD13, CD33 and CD34[10]. Depending on the morphological subtypes of AML and stage of differentiation block, other cells markers can be expressed such as megakaryocytes markers (CD41, CD61), erythroid (CD36, CD71) and monocytic differentiation markers (CD4, CD14 and CD11b [9]). Frequently, leukemic blasts express aberrant antigens, characteristic of other lineages such as CD19 or CD7 and that are useful in the identification of malignant cells.

The wide genetic heterogeneity of AML, increasingly recognized over the past 15 years, has been a barrier to therapies implemented until now[11].

According to the WHO Classification of Tumors of Hematopoietic and Lymphoid Tissues in 2008, the major categories of the classification for AML are: AML with recurrent genetic abnormalities, AML with myelodysplasia related changes, therapy-related AML and AML not otherwise specified. In 2016, WHO classification of Acute Myeloid Leukemia and related neoplasm has undergone

some changes and nowadays it is the most current classification which is outlined in Table 1. Myeloid sarcoma and myeloid proliferations related to Down Syndrome are the two new categories added [12].

Although cases of AML have an unknown etiology, some risk factors are known: age, male gender, family history, smoking, chronic myeloproliferative neoplasms and genetic syndromes. Other factors could influence and be considered as risk factors like exposure to the chemicals benzene and formaldehyde, high dose of radiation exposure, and chemotherapeutic drugs that have an active role in the origin of AML [7, 13].

Non-random chromosomal abnormalities, such as deletions and translocations are identified in roughly 52% of all adult primary AML patients and have long been recognized as the genetic events that cause and promote this neoplasm [14].

Table 1 - WHO classification of myeloid neoplasm and acute leukemia [12].

Types	**Genetic abnormalities**
AML with recurrent genetic abnormalities	AML with t(8:21)(q22;q229; RUNX1-RUNX1T1
	AML with inv(16)(p13.1.q22) or t(16;16)(p13.1;q22); CBFB-MYH11
	AML with PML-RARA
	AML with t(9;11)(p21.3;q23.3); MLLT3-KMT2A
	AML with t(6;9)(p23;q34.1); DEK-NUP214
	AML with inv(3)(p21.3.q26.2) or t(3;3)(p21.3;q26.2); GATA2-MECOM
	AML (megakaryoblastic) with t(1;22)(p13.3;q13.3);RBM15-MKL1
	AML with BCR-ABL2 (provisional entity)
	AML with mutated NPM1
	AML with biallelic mutations of CEBPA
	AML with mutated RUNX1 (provisional entity)
	AML with minimal differentiation
	AML without maturation
	AML with maturation
	Acute myelomonocytic leukemia

	Acute monoblastic/monocytic leukemia
	Acute erythroid leukemia
	Pure erythroid leukemia
	Acute megakaryoblastic leukemia
	Acute basophilic leukemia
	Acute panmyelosis with myelofibrosis
Myeloid sarcoma	Transient abnormal myelopoiesis
Myeloid proliferations related to Down syndrome	ML associated with Down Syndrome

Abbreviation: AML acute myeloid leukemia; APL, acute promyelocytic leukemia; ML, myeloid leukemia; WHO, World Health Organization.

1.2.1. Diagnosis

The diagnosis of AML can be complex and there is a need for an accurate risk stratification at presentation. Therefore, the studies performed in the workup of AML serve two purposes: firstly, to rule out other differential diagnoses and establish a definitive diagnosis of AML; and secondly to identify the AML subtype, to help risk-stratify the patient, predict prognosis, and formulate treatment strategies. After the classification of AML into a particular subtype, a final diagnosis is achieved. AML diagnosis is suggested by a complete blood cell count showing pancytopenia and blast cells and is confirmed by bone marrow examination. The diagnosis is made by the presence of ≥20% blasts in the peripheral blood or in the bone marrow or through the presence of unique genetic abnormalities found in the bone marrow regardless of blast count, namely t(8;21), inv(16), and t(15;17). Thereby, a bone marrow aspirate is the standard method for obtaining diagnostic samples. Peripheral blood can be used as an alternative to marrow for immunophenotyping and cytogenetic studies providing that there are significant numbers of circulating blasts. Fluorescent *in situ* hybridization, analysis of the expression of cell surface or cytoplasmic markers by flow cytometry, immunohistochemistry, and molecular mutation testing (ex. FLT3 mutation analysis) remain also essential for diagnosis, classification and risk stratification. These above-mentioned studies should be routinely used for initial diagnosis and performed during follow-up of AML.

Prognosis

An abnormal karyotype is observed in approximately 60% of patients but not all genetic abnormalities are synonymous of an adverse karyotype, as shown in Table 2)[15]. AML is classified into three prognostic risk groups: favourable, intermediate and adverse. About 25% of AML cases have cytogenetic abnormalities which predict a relatively favourable outcome. An adequate therapeutic approach in cases with genetic aberrations such as t(15;17), inv (16) / t(16;16) and t(8;21) are examples of AML with a favourable prognosis, with complete remission rates exceeding 90% and low relapse rates .

Nevertheless, roughly 10-20% of patients have genetic aberrations which result in a poor prognosis with low overall survival and complete remission rates of around 60%. This adverse karyotype normally includes monosomies of chromosomes 5 and 7 (-5/-7), deletions of 5q [del(5q)], abnormalities of 3q [abn(3q)], t(6;9)(p23;q34), t(9;22)(q34;q11), 17p deletions and a complex karyotype[16]. There are also entities of intermediate rist, not classifiable as favourable or adverse[9].

Others 40% of AML patients will have a normal karyotype which means that in these cases, cytogenetic analysis will be uninformative. However, an expanding range of molecular markers (mutations and gene overexpression) having prognostic significance has been identified. For example, mutated NPM1 without FLT3-ITD mutations is associated with a favourable prognosis[17]. Thereby, genetic analysis can be considered as the most powerful independent predictor of disease outcome in AML.

Table 2 - Risk Profile Categories as Determined by Molecular and Cytogenetic Abnormalities. Adapted from Blood 2017

Karyotype	Cytogenetic abnormality
Favorable	t(15;17)(q22;q21)
	t(8;21)(q22;q22); RUNX1-RUNX1T1
	inv(16)(p13q22)/t(16;16)(p13;q22)
	CBFB-MYH11
	Mutated NPM1 without FLT3-ITD/low FLT3-ITD
	Biallelic mutated CEBPA

Intermediate	Mutated NPM1 and FLT3-ITD (high) Wild-type NPM1 without FLT3-ITD/ low FLT3-ITD (normal karyotype) T(9;11)(p21.3;q23.3) MLLT3-KMT2A) Entities not classified as favourable or adverse
Adverse	t(6;9)(p23;q34.1); DEK-NUP214 t(v;11q23.3); KMT2A rearranged t(9;22)(q34.1;q11.2); BCR-ABL1 inv(3)(q21.3q26.2) or t(3;3)(q21.3;q26.2); GATA2,MECOM(EVI1) -5 or del(5q); -7; -17/abn(17p), Monosomal karyotype Wild-type NPM1 and high FLT3-ITD Mutated RUNX1 Mutated ASXL1 Mutated TP53 Complex (≥4 unrelated abnormalities)

1.2.1.1. Age as a clinical prognostic factor

Age is consistently a major unfavorable prognostic factor that affects both in terms of response and overall survival[18]. Improving anti-infective agents as well as reducing mortality associated with allogeneic stem cell transplantation may explain some improvement in the natural history of young adult individuals with AML. In general, 45-50% of patients under 60 years diagnosed are now cured. However, older adults (patients who are older than 60 years of age) need improved therapy, as a statistical data point to a probability of less than 20% of long-term survival[19]. The median survival of only 5 to 10 months for patients who are not able to receive intensive chemotherapy without unacceptable side effects remains dismal and very disturbing. In this sense, there is a great need to understand better the pathophysiological mechanisms involved and to develop more effective therapies.

1.2.2. Treatment

Untreated AML could be fatal over a period of days or even weeks depending largely on the level of the blast count in the peripheral blood and on the presence of complications of marrow failure or tissue infiltration[18].

The treatment of AML involves initial induction therapy and post-remission therapy. Induction therapy aims to achieve complete remission (CR) with preferably no measurable residual disease (MRD). Studies have demonstrated that induction therapy improves survival in patients who achieve CR regardless of the type of induction therapy [20]. Many factors determine which initial induction treatment should be chose. Some of those factors are the functional status of the patient, biological status of the disease, and goals of the patient. The two commonly used induction therapies in acute myeloid leukemia include cytotoxic chemotherapy with or without targeted therapies and hypomethylating agents with or withoutp target therapies.

On the other hand, post-remission therapy aims to prevent relapse of the disease. The two commonly employed strategies are additional post remission cytotoxic chemotherapies such as cytarabine (high or intermediate dose) with or without targeted therapies, or allogenic hematopoietic stem cell transplantation [21, 22]. The choice of therapy is determined by the unique risk and benefits provided by each treatment[23].

Despite 8 new treatments with different mechanisms of action (Midostaurin, CPX-351, Gemtuzumab Ozogamicin, Enosidenib, Ivosidenib, Venetoclax, Gilteritinib, Glasdegib) have also been approved for AML from 2017 to 2019, this aggressive hematopoietic disease with a poor prognosis and incurable 50 years ago, remains being a therapeutic challenge often due to the significant toxicity associated with those available treatments.

1.2.2.1. Secondary AML – Response to therapy

During the years between 1977 and 1995, the overall incidence of AML remained stable. However, over the years, there was a significant increase of

secondary AML, which appears in approximately a fifth of AML patients[24]. This risk remains particularly high as the population ages and as the result of other hematological disorders like myeloproliferative disease or among individuals with other cancers (e.g. breast cancer) exposed to chemotherapy (e.g. alkylating agents) and/or radiotherapy.

According to the nature of the agents that patients were exposed to, therapy-related AML was traditionally classified in two subgroups, which influence important disease characteristics, leading to a favorable or a poor prognosis[25-27]. In this sense, one of the classic subtypes of therapy-related AML is characterized by balanced translocations, particularly involving MLL at 11q23, RUNX1 at 21q22, RARA at 17q21 and NUP98 at 11p15 which are commonly developed as a consequence of the treatment with drugs targeting DNA topoisomerase II. Usually, this leukemia tends to appear 1,5 to 3 years after the first contact with the drug (short latency period), with no intervening myelodysplastic phase. On the other hand, treatment with radiotherapy, alkylating agents or anti-metabolites is associated with a leukemia characterized by a complex karyotype often by a high prevalence of TP53 mutation and featuring loss or deletion of chromosome 5q and/or 7[28-30]. Besides that, this type of leukemia is associated with a longer latency period, since this leukemia takes approximately 5 to 7 years to arise from the time of first drug exposure and might be preceded by a myelodysplastic phase.

Nevertheless, it has not been an easy task distinguishing these two subtypes of therapy-related AML since almost of patients who develop this clinical complication have been exposed to combination therapies which makes it harder to identify the main causative agent in both cases.

2. Angiogenesis

The first recorded scientific insights into the field of angiogenesis were provided by the Scottish anatomist and surgeon John Hunter in 1787 [31].

Angiogenesis can occur by two different mechanisms: sprouting and intussusceptive. When there is the formation of blood vessels in hypoxic tissues, i.e., in tissues lacking vascularization, the process is called sprouting

angiogenesis while intussusceptive angiogenesis, also known as splitting angiogenesis, happens when blood vessels are formed by the subdivision of existing ones [32, 33]. Thus, angiogenesis is defined as the ongoing vital process responsible for sprouting and forming new vessels from a pre-existing vessel network by endothelial cells (EC) under the guidance and balance of positive and negative angiogenic modulators within the vascular microenvironment [33, 34]. Thus, it requires the interaction between several biological components, such as angiogenic factors, extracellular matrix proteins, adhesion receptors, and proteolytic enzymes to define a hierarchical and functional vascular network.

From embryogenesis to postnatal life, angiogenesis which follows vasculogenesis – formation of vessels from endothelial precursors (angioblasts) – occurs at any time and any place where the physiological environment permits the increase and development of those blood vessels in a functional and standardized manner[35]. Thereby, this dynamic biological process plays an important role in the normal development of tissues and organs of all vertebrates. Normal angiogenesis is typically characterized by an architecture of vasculature well-organized and defined[36]. Any dysfunction in the formation of the vascular network leads to pathological events, including diseases such as neurodegeneration, aneurysms, proliferative retinopathies, cardiovascular diseases, cancer, among others. Indeed, one of the most common postnatal angiogenesis processes is the one induced by tumors, which allows a better comprehension of molecular mechanisms involved in the regulation of angiogenesis. The architecture of tumor vasculature is disorganized and is therefore sometimes inappropriate for some studies as the morphogenetic processes required for the construction of a hierarchical vascular architecture [37]. In diseases, a disrupted supply of oxygen and nutrients drives dysregulated angiogenic growth factors that influence angiogenesis, whereas dysregulation of angiogenesis also reciprocally disrupts the delivery of oxygen and nutrients, which results in a disturbed balance between metabolic demand and supply, thus compromising tissue function.

Approximately 100 000 miles of blood vessels give rise to the vasculature of adult human blood. The importance of this system lies in its role in supplying the body with oxygen and nutrients needed, the removal of carbon dioxide, some metabolic products and waste, and the circulation of cells and their products, especially hematopoietic cells allowing immune surveillance [35].

Likewise, for a tumor to grow beyond a certain size (≈2-3mm^3), is fundamental a network that provides the same conditions [38].

2.1. Angiogenesis in Acute Myeloid Leukemia

In 1863, Virchow first introduced the concept of tumor-induced angiogenesis. This concept was initially criticized by several researchers until Judah Folkman formulated the hypothesis that tumor growth is angiogenesis-dependent in 1971[38]. Based on a proposal that blocking angiogenesis could prevent the growth of solid tumors, reduce primary tumor volume and tumor metastasis, Folkman proposed anti-angiogenesis as a potentially promising new therapeutic approach for cancer treatment.

Tumor angiogenesis depends on the expression of specific mediators that initiate a cascade of events leading to the formation of new microvessels and is mediated by tumor-secreted angiogenic growth factors that interact with their surface receptors expressed on EC.

Nowadays, the importance of angiogenesis for the progressive growth and viability of solid tumors is well-established[37]. Likewise, data suggest an involvement of angiogenesis in the pathophysiology of hematologic malignancies, although the mechanism of bone marrow angiogenesis in hematological cancers seems to be more complex than tumor angiogenesis. The first studies to demonstrate an association between angiogenesis and acute myeloid leukemia were made by several research groups that reported increased angiogenesis through increased microvessel density (MVD) in bone marrow biopsies from patients diagnosed with AML[39-42]. That increased MVD resulted in a decrease in response to induction therapy, which was after restored to normal levels upon complete remission.

Vascular endothelial growth factor (VEGF), commonly referred to as VEGF-A, is one of the most studied angiogenic factors and promotes EC survival, proliferation, and migration, and increases vascular permeability and adhesion molecules on endothelial cells [43]. Leukemic cells express VEGF and its receptor VEGFR and thereby stimulate neovascularization in the bone marrow which results in an adverse prognosis in AML[44].

More recently, our group reported a differential bone marrow vascular remodeling in AML. Duarte et al. showed that while MVD was increased, bone-lining endosteal blood vessels were depleted in mice and patients with leukemia. By restoring blood vessels in the endosteum, it was possible to increase chemotherapy delivery and protect non-malignant hematopoiesis.

2.2. The Mouse Retina as an Angiogenesis Model

Animals have been used in studies and research for millennia in human history. The possibility of experimenting under controlled situations and mimicking biological conditions of human and animal diseases reinforced the development of scientific methods and the creation of the concept of animal biological models [45]. According to the objective of the investigation and associated with the advantages and disadvantages of its use, some species are more appropriate and used than others in animal experimentation. For more than a century, laboratory mice have been used as models for research into the genetic basis of human cancers. In fact, the laboratory mouse is still an experimental model of choice for analysis of a series of clinically relevant aspects of cancer biology. Advantages such as physiological and genetic similarity, easy manipulation and rapid reproduction, explain the frequent use of this animal model in biomedical research.

It is also fundamental to choose an appropriate vascular model to better understand the angiogenesis process as well models are required that accurately reflect the different biological steps that are involved. There are several animal models used to study angiogenesis. Mouse retina is an excellent model for studying angiogenesis *in vivo*.

The eye of the mouse (figure 2), like any eye, is one of the most complex and delicate structures of your body. Each structure that constitutes it has a specific role, which helps it carry out its functions. The retina, one of its constituents, has photoreceptors, as well as blood vessels that nourish it.

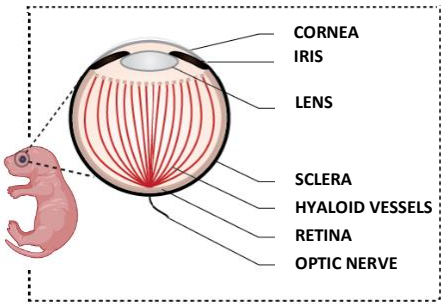

Figure 2 - Anatomy of the developing mouse eye.

Over the past decades, the mouse retina has been widely used as an angiogenesis model both on study of developmental and pathologic vessel growth *in vivo[46]*. For instances, in 1995, Keshet et al. used the mouse retina during developmental angiogenesis to analyze VEGF expression, and later, in 2002, the Stalmans laboratory explored the specific roles of different VEGF isoforms during retinal vascular development [47, 48]. Later, Holger and colleagues studied how VEGF-A controls angiogenic sprouting in the early postnatal retina and induces filopodial extension from specialized endothelial cells situated at the tips of the vascular sprouts [33]. In 2002, the Friedlander group had started investigating the role of bone-marrow stem cells in angiogenic development and suggested that vascular targeting of bone marrow-derived HSCs is dependent on mechanisms like those used by endogenous retinal vascular endothelial cells [49-51]. In 2009, the role of the Notch signaling pathway in vascular development was studied using the mouse retina by Rui Benedito et al[52]. Until now, many other research groups have used the retina model to study different aspects of angiogenesis.

Indeed, retina has been extensively used as an important tool in the understanding of vascular biology. One of the major benefits, of studying postnatal retinal development in mice lies in the ease of accessibility of the developing vasculature imaging and intervention without the difficulties associated with investigating embryonic development. There are other advantages associated with using this powerful experimental model such as:

- It is a useful model system to analyze the cellular and molecular processes involved in the construction of organized architecture, since the development process of the superficial vascular layer occurs after birth offering good conditions of visibility and manipulability of its processes. Thus, the

architecture of the vessel network and other processes such as endothelial cell proliferation, sprouting, vessel remodeling, or maturation can be analyzed at high resolution[53].

- Due to its two-dimensional or three-dimensional structure, the vascular network could be illustrated as a whole in flat-mount preparations, which facilitates its analysis[54].

- It is one of the few places in the body where blood vessels might be directly observed and analyzed in a physiologically relevant context and, as such, provides an opportunity to evaluate a specific parameter regarding other vascular systems.

- As postnatal vascular development in the retina proceeds in a very tightly regulated and organized pattern, it also allows to reliably detect any abnormality during development, both in transgenic animals and in pharmacologic studies [55].

In addition, as an organized vascularization is crucial not only for physiologic development of the retina but also for the normal and functional development of almost all tissues, many remarks in the developing mouse retina also apply to angiogenesis that it is inherent in the development of other organs. In this sense, the mouse eye has been used by many scientists to understand the mechanisms involved in developmental angiogenesis or tumor vascularization[56].

Furthermore, newborn mice develop a vascular network in a well-defined and patterned fashion that can be analyzed to study genetic and toxic manipulations. In fact, the retina provides an excellent model to study endothelial cells in detail and the vascular effect of compounds, including iron and iron-containing heme, in space and time.

2.1.1. Sprouting angiogenesis – Development of Retinal Vascular System

In contrast to the retinal angiogenesis in humans, whose retina starts vascularizing in utero at around 16 weeks of gestational age, a rodent such as mouse born blind. Thus, mice have no dedicated retinal vascular system before birth [57, 58]. Instead, they have persistent hyaloid vessels until birth [57, 58]. After birth (from postnatal day 1 - P1 in figure 3), the mouse retinal vascular system starts developing radially and sprouts from the optic disc, forming a primitive vascular plexus which is soon remodeled into small and large vessels. Over time it forms a superficial layer that establishes a hierarchical architecture consisting of distant arteries, veins and capillaries and continues progressively sprouting and extending until a complete two-dimensional vascular structure is formed (P2-P6). Later, as depicted in figure 3, a highly complex three-dimensional vascular system is formed from postnatal day 7 (P7) [46]. This network is interconnected by blood vessels that form new layers in deeper segments and provide the developing tissue with essential nutrients, oxygen and growth factors.

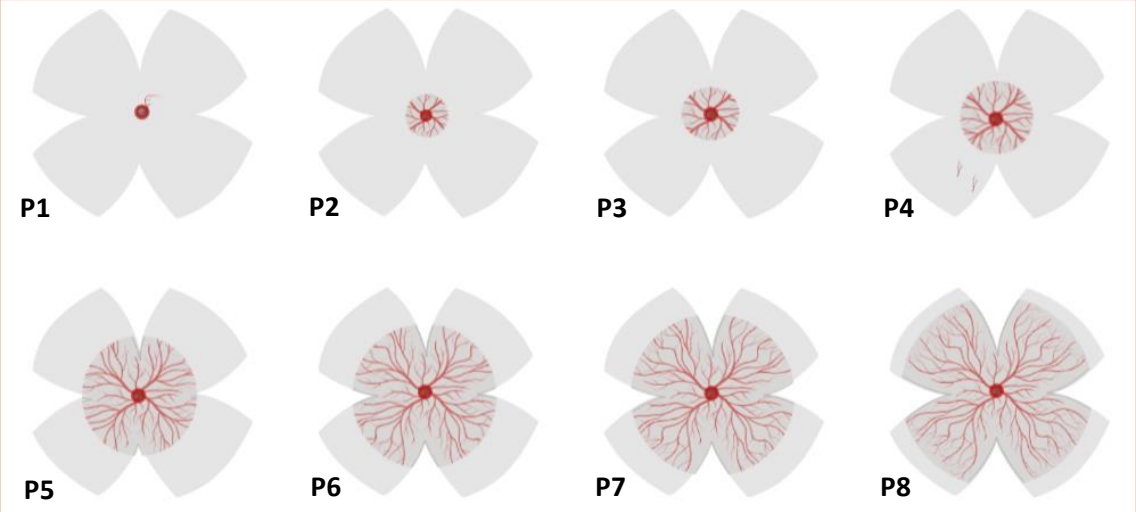

Figure 3 - Diagram of the development of mouse retinal vascular system from the birth of the mouse until eight day (P8). Immediately after birth, retinal vessels begin to sprout radially from the optic disc. The initially-formed primitive capillary plexus rapidly undergoes remodeling into large vs small, and arterial vs venous vessels [46].

The leading endothelial cell from a new vascular sprout is known as the tip cell. Tip cells produce filopodia and are followed by proliferating stalk endothelial cells. Thus, activated endothelial cells migrate and proliferate towards an avascular region where they form new blood vessels[59].

A chronological order of cellular development is requisite to obtain a proper formation of the retinal vascular system. The earlier component (tip cell) secretes growth factors required for the proliferation and migration of the succeeding components (stalk cells). Likewise, different components like astrocytes and mural cells establish cellular interactions with endothelial cells and play important roles in its development process. Astrocytes have a major function in inducing angiogenesis and absence of retinal astrocytes is coupled with absence of blood vessels in the retina [60]. Around embryonic day 17, astrocytes emerge from the optic nerve head and spread as a proliferating cell population in a centrifugal fashion across the inner surface of the retina, forming a cellular network that provides a template for the blood vessels. Thus, in P0 vascular endothelial cells start to sprout, guided by the preformed astrocytes network. In addition to the role of astrocytes, migration of smooth muscle actin-positive mural cells is also key, allowing sprouting endothelial cells, which eventually cover most vascular networks, except endothelial filopodia at the growing vascular edges[33] .

To study changes in the vascular architecture in small animals like mice, high-resolution equipment, such as confocal microscopy and 3D imaging can be. Furthermore, computational methods have facilitated the transition from observation-based histology to more quantitative measure. Some of the available software have high costs and require qualified professionals [61]. The open-access Image J software (including the FIJI package) appears as a free alternative that includes excellent plugins tailored for specific applications to trace and analyze features of the vasculature.

3. IRON

3.1. Iron biology

Iron is a crucial trace element in many enzymatic and metabolic processes, such as erythropoiesis, cellular respiration and oxygen transport to the various tissues of the body [62], DNA synthesis and repair, among others. Iron is also used in mitochondria for heme synthesis [63]. The average adult human has roughly 3-4g iron[64], and the major site of iron utilization is the bone marrow, where it is used in the synthesis of hemoglobin by red blood cell precursors. It is estimated that 200 billion erythrocytes are produced daily and, in order to maintain adequate erythropoiesis, more than 2×10^{15} iron atoms per second are needed[65] . The liver and spleen are the major storage organs for iron.

Two different forms of iron are known and can be obtained through diet: heme (~15% of iron in average diet) and nonheme (~85% of iron in average diet)[66]. Heme iron is easily absorbed in the intestine and is obtained from meat, poultry, and fish, while non-heme is essentially obtained by consumption of non-animal products, such as vegetables, cereals, bread and supplements and is not so efficiently absorbed in the intestine as heme iron[67-69] .

Mammals have developed mechanisms for keeping both cellular and whole-body iron concentrations within an optimal physiologic range. However, iron regulatory mechanisms are altered in some cases, which can cause iron overload or iron deficiency, depending on the pathway or process involved. It is already known that both iron deficiency and iron overload are harmful to humans. For example, iron deficiency is considered a global health problem that causes anemia (decrease in the number of red blood cells) and is associated with several problems, such as cognitive developmental defects and poor physical performance[70]. On the other hand, excess iron has also been associated with a negative impact. It affects parenchymal organs including the pancreas, liver, and heart. Iron overload might be toxic because highly reactive “free” iron readily accepts or donates electrons reacting with oxygen species (ROS), as superoxide and hydrogen peroxides that are continuously generated during the normal activity of cells living under aerobic conditions thereby producing the hydroxyl radical[64]. This hydroxyl radical formed in Fenton reaction is a highly toxic

reactant that leads to permanent modifications of target biological molecules, thus resulting in cell and tissue damage [71].

Equation 1

$$Fe^{2+} + H_2O_2 \rightarrow Fe^{3+} + OH^- + HO^{\cdot} \text{ (Fenton reaction)}$$

Most primary iron overload has a genetic basis[72]. Specific mutations in genes involved in the sensing of systemic iron levels (such as JJV, HFE, FPN, TRF2) can cause hemochromatosis [65].

To avoid iron deficiency and overload, iron availability is tightly regulated at both cellular and systemic levels. At the systemic level, hepcidin (a peptide produced by hepatocytes) regulates iron homeostasis by binding and degrading ferroportin (FPN). FPN is the only known cellular iron exporter and is highly expressed at the basolateral surface of duodenal enterocytes and on the cell membrane of macrophages. It controls the major fluxes of iron into blood plasma: intestinal iron absorption, the delivery of recycled iron from macrophages in spleen, and the release of stored iron from hepatocytes in liver. In this sense, due to the constant degradation of erythrocytes, conservation and recycling of iron are essential to replenish the iron contained within hemoglobin[73]. As mentioned above, this recycling process occurs primarily within the macrophage, which is capable of phagocytosing erythrocytes, with subsequent release of iron from heme by an enzyme called heme oxygenase-1 (HO-1)[74]. Thus, iron balance is maintained by limiting its intestinal uptake and by continuously recycling and reusing cellular iron. Iron binds the iron-transport protein transferrin and is distributed to tissues through blood plasma which contains only 2-4mg iron (figure 4)[64]. The hepcidin-ferroportin axis is therefore essential to maintain iron homeostasis [63]. Iron itself modulates hepcidin. In a situation of excess iron, hepcidin expression is increased, which then causes hypoferrinemia. In contrast, iron deficiency leads to low hepcidin and active iron release to the plasma.

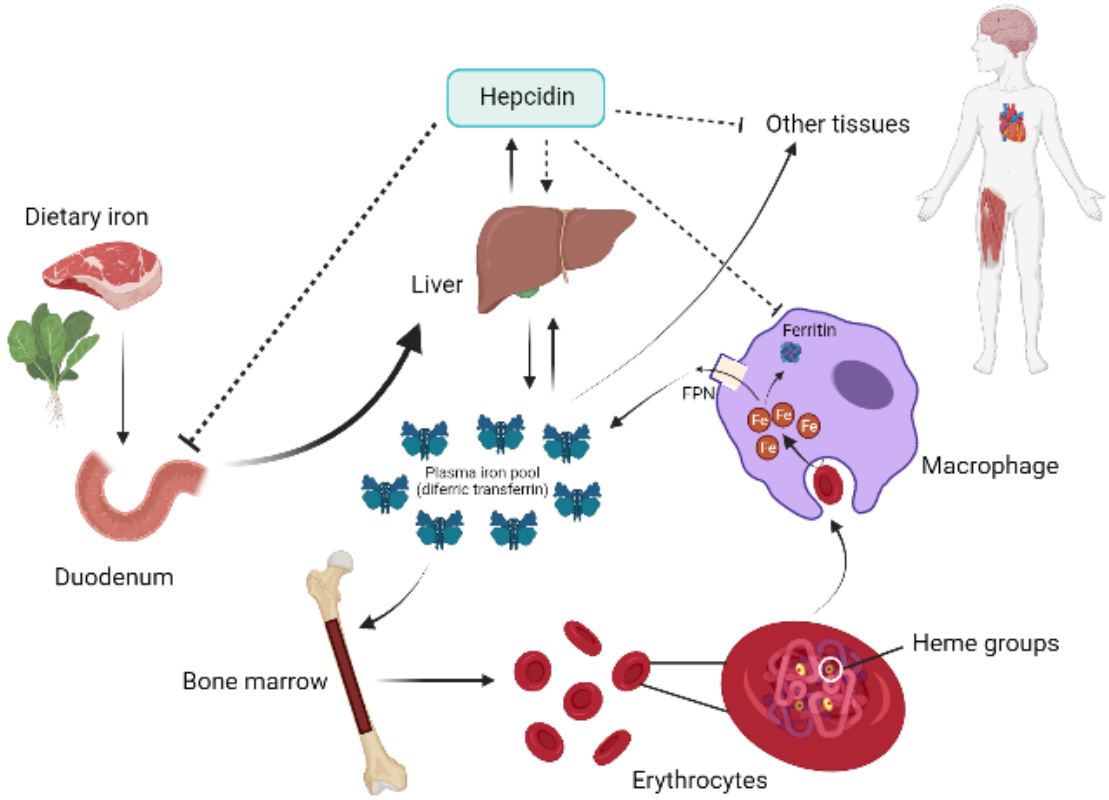

Figure 4 - Major iron flows and their regulation by hepcidin and ferroportin. Hepcidin controls the iron flow into plasma by inducing the endocytosis and proteolysis of the iron exporter ferroportin. Recycling process occurs primarily within the macrophage, which is capable of phagocytosing erythrocytes, with subsequent release of iron from heme.

3.2. Role of Iron in AML

Although iron is essential for multiple cell functions, it is also a pro-oxidant, thus contributing to the formation of free radicals that cause oxidative stress and lead to DNA damage. Derangement of iron metabolism at the systemic and/or cellular level may accompany common pathological events such as infections, inflammatory and metabolic disorders, neurodegeneration, and cancer. Iron plays an essential role in tumor progression and metastasis formation since it plays an active role in the survival of tumor cells and reprogramming of the tumor microenvironment [75]. Hereditary hemochromatosis – inherited iron overload disorder characterized by excessive absorption of iron – is associated with several forms of human carcinomas in the

liver, colon, and lung, hence establishing the principle that iron can promote cancer development. Although the metabolism of iron is altered in various types of cancers, it has been poorly explored in acute myeloid leukemia.

In 1994, the Adamson group showed that multiple red-blood-cell transfusions could increase the systemic iron pool in patients with leukaemia[76]. Deferoxamine, also known as desferrioxamine is an iron-chelating agent used to remove excess of iron from the body, usually caused by blood transfusions in adults. Deferoxamine chelates iron from intra-lysosomal ferritin and siderin forming a water-soluble chelate excreted by the kidneys and in the feces via the bile, known as ferrioxamine. Duarte et al., suggested that the deferoxamine molecule helps to preserve the endosteal endothelium, thus rescuing the loss of hematopoietic stem cells (HSCs). However, the mechanism underlying this vascular remodeling remains unknown[77].

Callens et al., have reported that leukemia is susceptible to ferroptosis, a new form of non-apoptotic cell death mediated by an excessive degree of iron-dependent lipid peroxide[78, 79]. After that, Yan Du and his research group recently demonstrated that ferroptosis is involved in the ATPR treatment via ROS-autophagy-lysosomal pathway, and its inhibition by specific drugs contributed to ATPR-induced AML cells differentiation [80].

Lopes et al., have recently demonstrated that AML is a complex pathology with unique iron profile not associated with inflammation or transfusion and characterized by high ferritin, low transferrin, high transferrin saturation (TSAT) and high hepcidin. According to this recent research, elevated TSAT at diagnosis is independently associated with increased overall survival in AML, thus suggesting TSAT as a relevant prognostic marker in AML. Furthermore, AML cells were shown to accumulate iron [81].

In addition, in a large series of AML patients submitted to intensive chemotherapy, about 10% of those patients showed very high serum ferritin levels and bone marrow hemophagocytosis[82], among other clinical alterations.

Gasparetto et al., has demonstrate that low level expression of ferroportin in AML is correlated with good risk cytogenetics and better outcomes, in part possibly due to an increased sensivity of FPN^{low} to chemotherapy[83].

More recently, Chan et al. showed the ability of iron to promote radiation-induced AML (RI-AML) in B6D2F1 mouse models.

Some retrospective reviews also suggested that iron overload in myelodysplastic syndromes – clonal disorders intrinsically linked to AML development – might promote the development of AML[84].

Despite the aforementioned data about iron playing a role in AML, there is still much to explore and understand about iron metabolism in this disease and its therapeutic potential.

3.2.1. Serum Ferritin in AML as a prognostic marker

In the 1930s, ferritin was discovered, a multi-functional protein with 24-subunit and two decades later, Addison et al., demonstrated that ferritin could be detected in human serum. Serum ferritin (SF) is generally known to be a good surrogate of human iron stores[85]. As mentioned before, excess iron and lack of iron can play a role in many diseases' development. In this sense, serum ferritin is widely used in diagnosing and monitoring these diseases[86]. Some studies have demonstrated that most of AML patients, including younger patients, have elevated serum ferritin levels at diagnosis even without no red-blood-cells transfusion at the time of diagnosis[87]. Other studies have also reported that ferritin has a negative prognostic impact in AML patients as showed by Tachibana et al. Lebon et al., reported that hyperferritinemia was significantly associated with a higher cumulative incidence of relapse as well poorer disease-free and overall survival[88, 89]. Ferritin regulates several biological processes at both extra and intracellular levels that could be relevant in AML biology including cell proliferation, immunosuppression, angiogenesis and chemoresistance [90].

3.3. Iron and retina

In the last 20 years, our knowledge about the mechanisms that control cellular and systemic iron homeostasis substantially increased. A key tool was the analysis of mice with either spontaneous variants or genetically engineered mutations in genes that affect iron metabolism. Many of the genes that regulate

iron on the systemic level are expressed in the retina and might play a role in local iron regulation[69].

De Jong mentioned that two-hundred years ago, it was discovered that, after dissection, the residual ashes of an aged human retina could be mobilized by a magnet [91]. Currently, in spite iron plays a main role in retinal physiology, it is known that excess of iron cause retinal degeneration and leads to loss of its function. Once again, iron chelation therapy could be used to prevent retinal degeneration.

In addition, although the retina might be safeguarded by the blood-retinal barrier, it is known that photoreceptors are damaged by excess iron, and as such, it is important to understand if the blood-retinal barrier can support in protecting against high serum iron levels. Zhao et al., studied if retinal iron accumulation in Bmp6 knockout mice might result from the high serum iron levels or alternatively, low levels of retinal hepcidin, an iron regulatory hormone whose transcription can be up-regulated by gene Bmp6[92].

It is also reported that iron level varies during retinal development and aging. As an example, a study made by Moss et al., has shown that in rats, iron entry is very high during retinal development and maturation, then decreases in adulthood, and increases again with aging[93].

4. NRF2

Oxidative stress due to imbalance between reactive oxygen species production and detoxification, plays a decisive role in cell fate. In response to the excessive ROS, apoptotic signaling pathway is activated to promote normal cell death [94]. ROS which includes hydroxyl radical (OH·) and superoxide anion radical (O2·-) and non-radicals as hydrogen peroxide, play a pivotal role in regulating the redox signaling pathway and can affect the vasculature in a dose-dependent manner [95, 96]. Long-term production or high concentration of ROS due to unbalanced generation and elimination under pathological conditions damage the vascular system. On the other hand, moderate ROS can promote angiogenesis and tissue regeneration in physiological conditions[97]. Oxidative stress can destroy biological macromolecules such as lipids, proteins, nucleic

acids among others, leading to aging and age-dependent diseases including cancer[98].

As already mentioned, iron is involved in many redox reactions that are required for enzymatic catalysis and electron transfers. Thus, increased iron levels inducing oxidative stress activate the transcription factor Nuclear factor erythroid 2-related factor 2 (Nrf2)[99].

Nrf2 is an intracellular transcription factor that regulates the expression of a number of genes to encode anti-oxidative enzymes, anti-apoptotic proteins, detoxifying factors, and drug transporters. In this sense, Nrf2 is highly sensitive to oxidative stress and protects cells via binding to the antioxidant response elements in the nucleus and promotes the transcription of a wide variety of antioxidant genes. It is documented that Nrf2 is implicated in many cancers' biology, despite the existence of some controversies. It has been suggested that Nrf2 is able to participate as an oncogene in cancer development or a tumor suppressor though cancer preventive signaling pathways[100]. Sporn et al., suggested that Nrf2 is activated in order to protect normal cells from harmful oxidative products whereas, constitutively activated Nrf2 is associated with promoting cancer growth and decreasing sensitivity to chemotherapy[101].

Heme oxygenase-1 (HO-1) is a Nrf2 regulated gene that plays a critical role in the prevention of vascular inflammation[102]. Moreover, HO-1 metabolizes cytosolic heme from red blood cells into ferrous iron and biliverdin, thus allowing the recycling of ferrous iron for fresh erythrocyte production.

Regarding Nrf2 role in AML, Karathedath et al., demonstrate Nrf2 as an intrinsic druggable target in AML, and suggested the possibility of using Nrf2 inhibitors in combination with chemotherapeutic agents with the objective to modulate drug resistance in AML[103].

5. Human Plasma, Bone Marrow Fluid and Peripheral Blood Mononuclear Cell Isolation with SepMate

Peripheral blood mononuclear cells (PBMCs), also known as human mononuclear cells, refer to any blood cell carrying a rounded nucleus, such as lymphocytes (T cells - group with higher %, B cells and NK cells), macrophages

and monocytes. These cells can be extracted from whole blood through a centrifugation by density gradient (separation of the particles at different densities) with Ficoll, a hydrophilic polysaccharide that separates layers of blood. In this way, it is possible to separate blood into an upper layer, plasma, followed by a lower layer of PBMCs and a fraction of polymorphonuclear cells such as neutrophils and eosinophils, followed by a thin layer of granulocytes, and finally a lower layer of erythrocytes, since they have the highest density of all components (figure 5).

The method for extraction of peripheral blood mononuclear cells using Ficoll was first described in 1968 [104]. Since then, some alternative methods of gradient isolation have been developed with the aim of optimizing the entire process, from the time spent, to the handling of the samples, and also to avoid contamination with other cell types and to minimize any unwanted activation of the isolated cells. It was in this sense that, as an alternative to the classical Ficoll approach, 50 mL SepMate™ tubes were developed - innovative tubes that allow the consistent and trouble-free isolation of PBMCs.

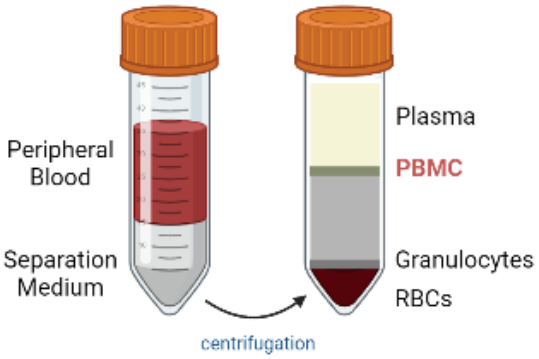

Figure 5 - Representative illustration of layer separation, typical result using density gradient after centrifugation. Adaptated from: Cell Aplications, INC, Human Peripheral Blood Mononuclear Cells: PBMC/HMNC-PB

6. Aims

We hypothesize that the AML-induced remodeling of the endosteal vascular niche are a consequence of the toxicity caused by excessive local iron. In order to study the *in vivo* effect of iron on endothelial cells, the present research project will focus on the exploration of an alternative model to study blood vessels - the retinal angiogenesis model. Preliminary data show that endosteal endothelial cells do not correctly express heme oxygenase-1 (Hmox1), which is downstream of the master antioxidant transcription factor Nrf2. Therefore, we will evaluate the consequence of endothelial-specific deletion of Nrf2 in the vascular response to iron toxicity. Altogether, we aim to use the well-described retinal angiogenesis model to study the *in vivo* iron-induced damage of endothelial cells and the putative role of Nrf2 in this process. This study can have wider implications in understanding the mechanisms driving the remodeling of the vascular niche in acute myeloid leukemia and in demonstrating the role of endothelial Nrf2 antioxidant responses.

In this sense, this research project will focus on these two main aims:

- **Does exposure to free iron (as observed in AML) induce an increase in the in vivo vascular permeability?**

- To evaluate the permeability of retinal blood vessels when exposed to iron.

- **Is Nrf2 mediating the susceptibility of endothelial cells to iron in vivo?**

- To evaluate the phenotype, morphology, and permeability of retinal blood vessels of endothelial-specific Nrf2 knock-out mice (Cdh5-CreER; Nrf2-floxed).
- To evaluate the phenotype, morphology, and permeability of retinal blood vessels of endothelial-specific Nrf2 knock-out mice (Cdh5-CreER; Nrf2-floxed) when exposed to iron.

I also intend to isolate bone marrow and peripheral blood mononuclear cells from leukemia patients in order to quantify ferritin and thus evaluate potential local differences in iron storages in AML.

CHAPTER 2. MATERIAL & METHODS

1. Human plasma, bone marrow fluid and peripheral blood mononuclear cell isolation with SepMate

BM aspirate and peripheral blood from patients were collected into tubes containing EDTA after informed consent and processed in our laboratory. Collection tubes were centrifuged at 200g for 10 minutes at 20°C and then, the supernatant (BM fluid and plasma) was carefully removed by transferring the top 2mL into a 15 mL falcon tube. The isolated plasma and BM fluid was centrifuged at 1,000g for 10 min at 20°C, aliquoted into Eppendorf tubes (200µl/vial) and stored at -80°C for future analysis. 2ml of sterile PBS was added to the tubes containing mononuclear cells. 15ml of Ficoll/Histopaque (density gradient medium) were added to a 50ml SepMate™ falcon by carefully pipetting it through the central hole of the SepMate™ insert. The whole blood was transferred to a new 15 ml falcon tube, resuspended in 15ml of PBS and transferred to the SepMate™ tube by slowly pipetting it down the side of the tube, layering on top of the Ficoll layer. The tube was then centrifuged at 1200g for 10 min at room temperature. After centrifugation, the top layer enriched in PBMCs (figure 6) was carefully transferred into a new 50 mL falcon tube. PBMCs were washed twice by resuspending the cells in 50mL PBS (centrifugation at 1200rpm for 6 min at room temperature). Viable cells were counted using the trypan blue exclusion method and a hemocytometer. On average, 50 x 10^6 viable cells are expected for the peripheral blood samples and twice the cells in the BM samples.

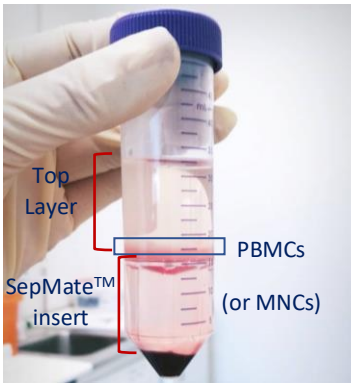

Figure 6 – Isolation of PBMCs using SetMate™ tubes.

PBMCs were cryopreserved immediately after isolation using a freezing medium containing 10% cryoprotectant intracellular dimethylsulfoxide (DMSO) plus 90% Fetal Bovine Serum (FBS). For long-term storage, the vials are placed in a Mr. Frosty™ Freezing Container at -80°C and then transferred to the liquid nitrogen. It is also important to mention that the samples must be properly identified, with patient code, type of sample - peripheral blood (PB) or bone marrow (BM), vial number, researcher, and date.

The study was reviewed and approved by Instituto Português de Oncologia do Porto's Local Ethics Committee (approval 158/018).

2. Mouse experiments and procedures

All protocol for animal experiments were performed after approval by the IBMC/I3S Animal Ethics Committee and the national authority Direção-Geral de Alimentação e Veterinária (DGAV). *Mus musculus* C57Bl6/J female and male newborn mice were used and generated at the animal facility of Instituto de Investigação e Inovação em Saúde. Cdh5(PAC)-CreERT2 mice were a gift from Dr. Ralf Adams (Max Planck Institute for Molecular Biomedicine, Germany). Nrf2-flox mice were acquired from The Jackson Laboratory. Animals were kept with high welfare standards and properly treated and monitored.

2.1. Mouse Cre/loxP system

Mice were genetically manipulated through the Cre/LoxP-mediated recombination system. Administration of drugs such as tamoxifen (T) in mice and its interaction, in cytoplasm, with the estrogen receptor (ER) containing a mutated ligand-binding domain (ER-LBD), leads to the disruption of the heat shock protein (HSP90) with the fused protein Cre recombinase, called CreER and, consequently, induces the activation and nuclear translocation of the complex CreERT. Cre recombinase is one of the tyrosine site-specific recombinases that plays a role in the recognition of 34bp-specific DNA fragments known as the loxP site and which mediates site-specific deletion of DNA sequences between two loxP (figure 7)[105, 106]. Cre-loxP system requires one mouse carrying a

Cre gene-directed and another mouse having alleles flanked by loxP (floxed) in the gene of the interest. In the absence of Cre, the targeted gene – Nrf2 in this case - will remain intact. Nrf2 conditional deletion is obtained by placing the Cre recombinase under the control of a tissue-specific promoter which is, in the current study, Cadherin 5 or VE-Cadherin (Vascular Endothelial Cadherin) - a transcription factor specific to the endothelium. In this experimental work, conditional knockout mice were generated by crossing the Cre-driver strain with a floxed mouse strain, thus obtaining a knockout mouse model with specific endothelial deletion of the Nrf2 gene (*Nfe2l2*), in exon 5, in order to evaluate the consequence of Nrf2 deletion in the vascular response to iron toxicity.

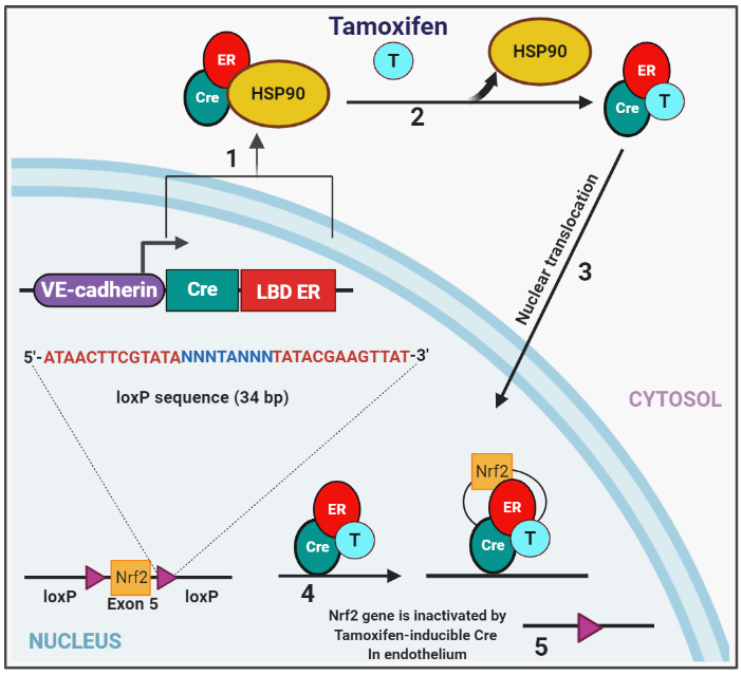

Figure 7 - The Cre/loxP system. CreER is a tamoxifen-inducible Cre recombinase fused to the estrogen receptor (ER). The expression of CreER fusion gene is triggered by an endothelial cell-specific promoter, Ve-cadherin. Upon exposure or contact with an exogenous inducer, Tamoxifen, the complex CreERT is translocated into the nucleus, where it recombines loxP sites and flank the target gene, Nrf2.

2.1.1. **Experimental Groups**

New-born Cdh5(PAC)-CreERT2 mice were genotyped by the Cell Culture and Genotyping Service of i3S after being sacrificed by decapitation at post-natal

day 5 (P5). $Nrf2^{lox/lox}$ and $Nrf2^{lox/+}$ mice were used as control ($Nrf2^{flox}$). Experimental $Nrf2^{i\Delta EC/+}$ mice were obtained by crossing Cdh5(PAC)-$CreERT2^{T/+}$ with $Nrf2^{lox/+}$. For genotyping, a PCR was made to detect Cre and Nrf2-floxed. The PCR mixture (10µL V/tube) for Cre contained 0.5µL of DNA, 0.5µL of forward primer VE-iCRE and 0.5µL reverse primer VE-iCRE, 3.5µL of H_2O (commercial) and 5µL of Bioline MasterMix. Regarding PCR mix performed for Nrf2, in addition to the other components, forward primer Nfe30131 and reverse primer Nfe30131 were used in the same concentration. The following step was to detect the presence of products amplified by agarose gel electrophoresis in all mice (Table 3). In Table 4 it is possible to see examples of the bands in agarose gel electrophoresis achieved to analyze the mouse genotypes.

Table 3 - Bands that might be detected after amplification of the PCR products by agarose gel eletrophoresis for Cdh5 and Nrf2 genes.

Cdh5-Cre	KO	=720 bp band	
	Heterozygote	=720 bp band	
	Wild type	No band	
Nrf2	Heterozygote	~310 bp band	
	Mutant	=272 bp band	~310 bp band
	Wild type	=272 bp band	

Table 4 - Bands obtained after products amplification in agarosis gel electrophoresis.

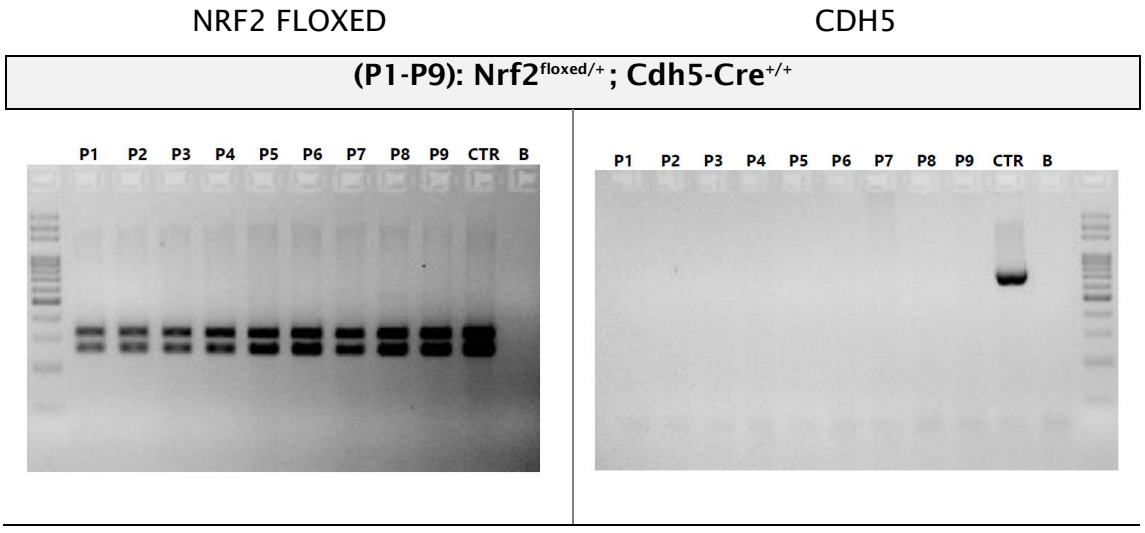

(P1; P4-P6): Nrf2$^{floxed/+}$; Cdh5-Cre$^{T/+}$ & (P2-P3):Nrf2$^{floxed/floxed}$; Cdh5-Cre$^{+/+}$	
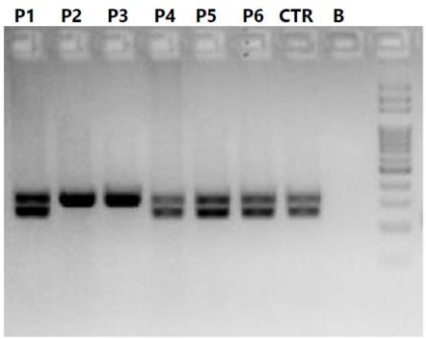	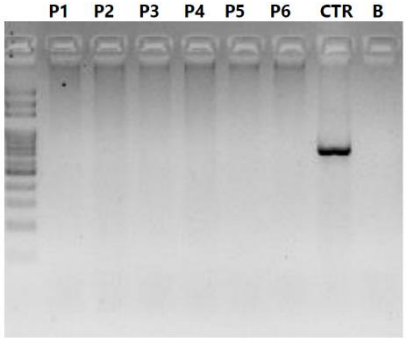

After genotyping, two genotypes were obtained (Table 5) and then pups were divided into four groups according to table 6.

Table 5 - Genotypes obtained by Cre-loxP system and its designation.

	GENOTYPE	DESIGNATION
Control	Nrf2$^{lox/lox}$ or Nrf2$^{lox/+}$	Nrf2^{flox}
EC-specific KO	Cdh5(PAC)-CreERT2$^{T/+}$;Nrf2$^{lox/+}$	Nrf2$^{i\Delta EC/+}$

Table 6 - Genotypes obtained by Cre-loxP system. Each pup didn't receive any treatment (C) or was injected with only Tamoxifen (T) or Tamoxifen plus Iron (T+I) and, at post-natal day 5, all were sacrificed to perform the retina dissection.

			STRAIN	
			Nrf2^{flox}	Nrf2$^{i\Delta EC/+}$
TREATMENT	n biological	No treatment	5	-
		Tamoxifen	8	-
		Tamoxifen + Iron	6	13

2.2. **Tamoxifen injections**

At post-natal day 1 (P1), pups were injected intraperitoneally with 20 µL of tamoxifen using a 0,3 mL insulin syringe for accuracy. To prepare the tamoxifen solution, 5mg of Tamoxifen (Sigma, cat# T5648) were weighed, 125 µL of absolute alcohol (100%) added and all mixed rigorously by shaking to dissolve any crystals present. Finally, 875 µL of peanut oil was added and when necessary the mix was incubated at 37˚C for 5 minutes to further dissolve the solution. Tamoxifen is light sensitive and should be prepared and stored at 4˚C until a maximum of 3 days in eppendorf wrapped in aluminium foil.

2.3. **Iron dextran injections**

At post-natal day 4 (P4), each pup from group 2 were injected intraperitoneally with 25 µL of iron dextran (Sigma, Cat# D8517). A solution of iron dextran was prepared 30 minutes before injections with 300 µL of iron dextran plus 700 µL of saline solution and at the end filtered with 0,2 µL to sterilize.

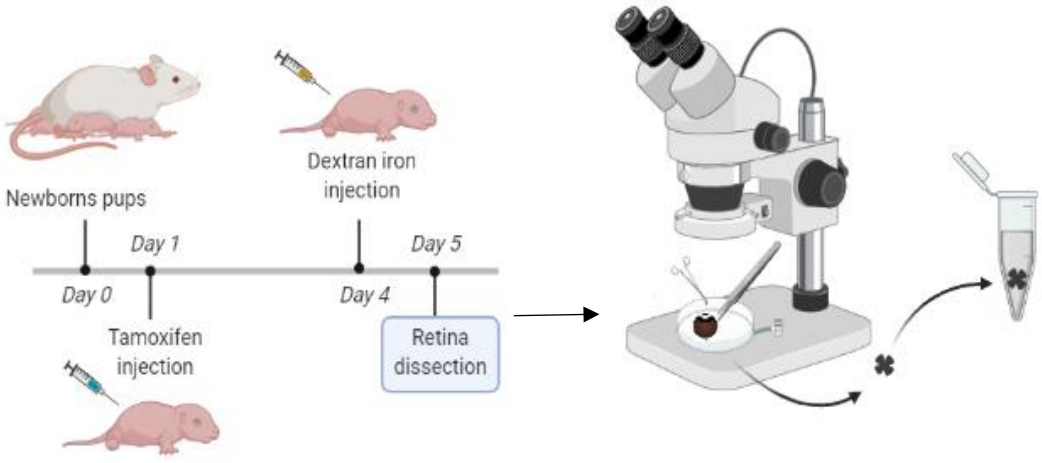

Figure 8 - Experimental design performed on mice for all genotypes. At postnatal day 1 pups were injected with Tamoxifen and at day 5 with Dextran Iron. On the following day, retinas were dissected using a stereoscope.

2.4. **Dissection of Postnatal Pup Retinas**

Upon decapitation at post-natal day 5 (P5), the skin membrane covering the newborn's eye was cut using a spring scissor (Fine Science Tools, No. #91501-09). Eyes were carefully collected using a curved tweezer (Fine Science Tools, Cat. #11274-20) and a fine forceps (Fine Science Tools No. #11254-20) and immediately fixed for 3 hours at 4˚C in a 2mL eppendorf tube with 4% paraformaldehyde (PFA). 4% PFA was prepared by dissolving 40g in 1L of PBS. After that, PFA was replaced by PBS for five washes and kept in PBS at 4˚C until further processing.

On the same day, using a stereoscope, the newborn's eyes were dissected in a Petri dish (figure 8) filled with a drop of PBS. The first step was cleaning of the connective tissue that surrounded the eye and puncturing the retina at the limit between the cornea and the sclera with a 26G needle. Then, it was necessary to hold the eye using a pair of fine forceps and, with extra care, remove the cornea, iris and lens. In the end, the sclera was also removed, as well as the hyaloid vessels and the optic nerve. After that, four radial incisions were performed on the isolated retina with the help of spring scissors (Fine Science Tools, No. #91501-09). Extracted retinas were embedded in PBS until the following step – immunofluorescence staining.

2.5. **Immunofluorescence staining of the Pup Retinas**

Immunofluorescence staining was performed for each extracted retina. The following commercial antibodies were used for immunostaining purposes: the primary antibody TER-119 to label erythroid cells and the secondary antibody Streptavidin-Phycoerythrin (PE) (Table 7). Retinas were permeabilized in 500 µL blocking buffer (0,5% Triton, 0,01% sodium deoxycholate, 1%BSA, 2% FBS, 0,02% sodium azide in PBS) for 2h, at room temperature (RT), and after that, the primary antibody (TER-119; diluted in 1:1 solution of PBS: Blocking buffer), was incubated overnight at 4˚C. On the second day, the retinas underwent three multiple washes with 1mL of PBS supplemented with 0,1% Tween-20 (PBS-T) for 30 minutes at room temperature. Secondary Streptavidin-PE was added (1:1000

dilution in 1:1 solution of PBS: blocking buffer) for 2h, at RT. Retinas were equilibrated with Pblec (Boston BioProducts, Cat# BM-731), 400 µL at room temperature, for 30 minutes. After three further washes with PBS-T, the retinas were stained with isolectin B4 conjugated with Alexa Fluor 488 at 1:400 (diluted in Pblec) overnight at 4˚C. In the following day, three more washes were done, and retinas were fixed with 500 µL of 1% PFA in PBS at room temperature for 15 minutes.

Table 7 - List of antibodies used for immunofluorescence staining in mouse retinas.

	Antibody	**Host**	**Dilution**
Primary antibody	TER-119	Anti-mouse	1:100
Secondary antibody	PE		1:1000
Isolectin	GS-IB_4 Alexa Fluor 488	-	1:400

Finally, retinas were carefully transferred onto glass slides using a Pasteur pipette, removing the excess of PBS-T with absorvant tissue. Retinas were mounted by adding drops of Faramount Mounting Medium (Dako, No. S3025) onto a coverslip and slightly positioning over the retina. Excess of mounting medium was removed from the edges of the coverslip. Then, a small amount of clear nail polish was added to the corners of the coverslips to prevent sliding of the retinas. A layer of electrical tape with windows cut with a scalpel was placed in the slide before the retinas were mounted, in order not avoid crushing the retina and to conserve the 3D architecture of the tissue. The retinas were placed overnight at 4˚C and protected from light.

This procedure is designated as Indirect immunofluorescence and as it was mentioned, involves two incubation periods. The first part consists of binding a non-labelled primary antibody to the target and then a second fluorophore-labelled antibody detects and binds to the Fc portion of the primary antibody (Figure 9)[107].

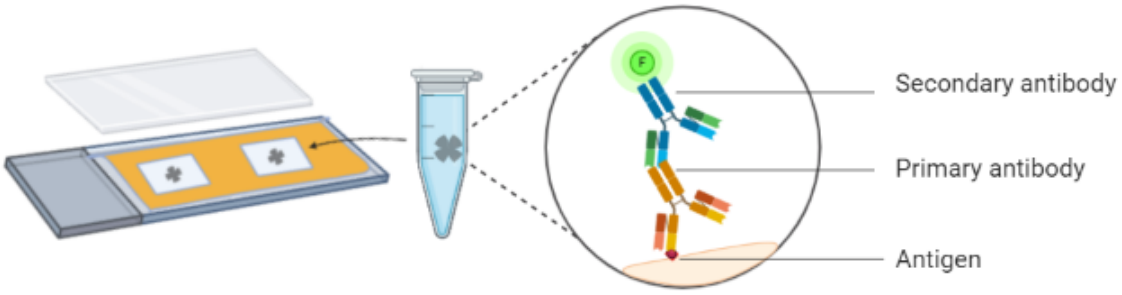

Figure 9 - Scheme illustrating the indirect immunofluorescent staining performed and the retina mounting way.

2.6. **In vivo retina imaging and image analysis**

Confocal microscopy and image analysis enable the visualization and quantification of the complex retinal vascular architecture in a minutely and comprehensive way [108]. In this respect, all retinas were imaged on a confocal laser-scanning microscope (Leica SP5 II) with a 10x magnification objective across LAS AF software. Once all parameters were configured and optimized, such as necessary lasers and their respective laser power, detectors for Leica/Alexa 488 and Leica/DSRED, format (frame resolution of 1024x1024 pixels), speed (400Hz), line average (3), a Z-stack in live mood, whose z-step was 8.99µm, and a Tile Scan were acquired. The Tile Scan allows bounding of the region of interest – the image of the whole retina – and the Z-stack allows recording images of the retina at different focal planes, where the entire sample volume can be rendered and visualized.

Retina images obtained through confocal microscopy were processed and analyzed using Fiji/Image J. Fiji is a useful software that allows the assessment of certain parameters as the number and length of blood vessels present in the retina like veins and arteries using the tool ROI Manager, and its vascular density by thresholding the IB4 staining in a part of the vascular network bounded in Fiji. Is also practical for a qualitative assessment of these vessels, for example, to verify the presence of microhemorrhages.

.

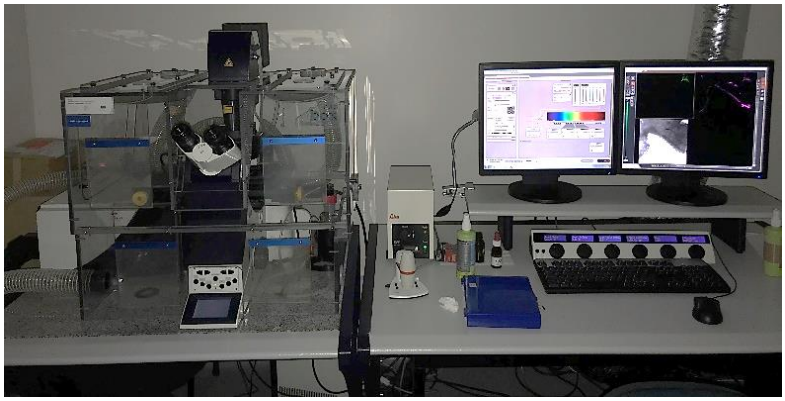

Figure 10 - Confocal laser-scanning microscope - Leica SP5 II used to image the retinas.

2.7. **Statistical analysis**

All statistical analyses were performed using GraphPad Prism 8.0.1 (GraphPad Software). All results were presented as mean ± SD. Unpaired Student's t-test was used to compare group means and one-way ANOVA followed by Tukey's post hoc test was used for multiple comparisons. Some statistical results were also performed using Wilcoxon-Mann-Whitney test. Statistical significance was considered at a p value <0,05.

CHAPTER 3. RESULTS

1. Ferritin Assay

After isolating human plasma, bone marrow fluid, and peripheral blood mononuclear cells from samples of AML patients, ferritin values were measured in both plasma and bone marrow for each patient. Ferritin was determined by immunoturbidimetric assay, using Olympus reagents and analyzer (Olympus Diagnostics). The quantifications were performed by Dr. Maria José Teles (Centro Hospital Universitário São João). Figure 11 shows the paired comparison of those measurements. As shown, AML patients have significantly higher ferritin concentrations in the bone marrow in comparison to the plasma. Additionally, although the range of ferritin concentration values in narrow in the plasma (between 592,1 ng/ml and 1695,4 ng/ml), they are quite heterogeneous in bone marrow fluid, ranging from 784.5 ng/ml to 8507.2 ng/ml.

We hypothesized that the local increased iron concentration in the bone marrow might contribute to the susceptibility of vascular endothelial cells. I therefore established the retinal angiogenesis mouse model to explore the *in vivo* effect of iron and the role of the master regulator of cellular anti-oxidant response, Nrf2 on endothelial cells.

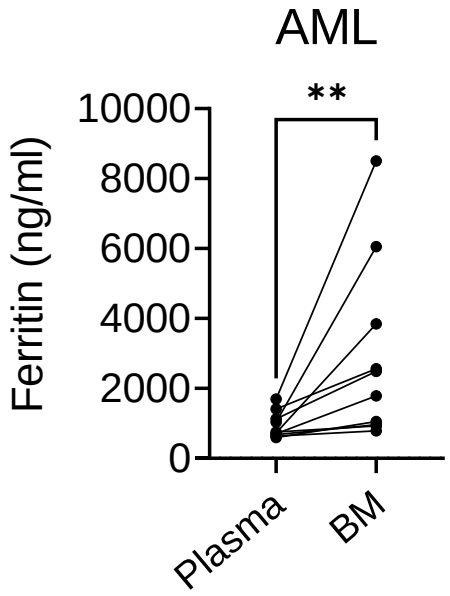

Figure 11 – Ferritin quantified in human plasma and bone marrow of 10 AML patients from IPO-Porto. See in attachment, table 9 to observed in more detail the values obtained.

2. Anatomical features of the retinal vasculature

To obtain retinas, I troubleshooted its dissection and isolation. After removing the cornea (figure 12A), the lens is also removed, as shown in figure 12B. After careful dissection, the retina is radially sectioned into a four-leaf clover shape to enable the whole mount, as is shown in figure 12C.

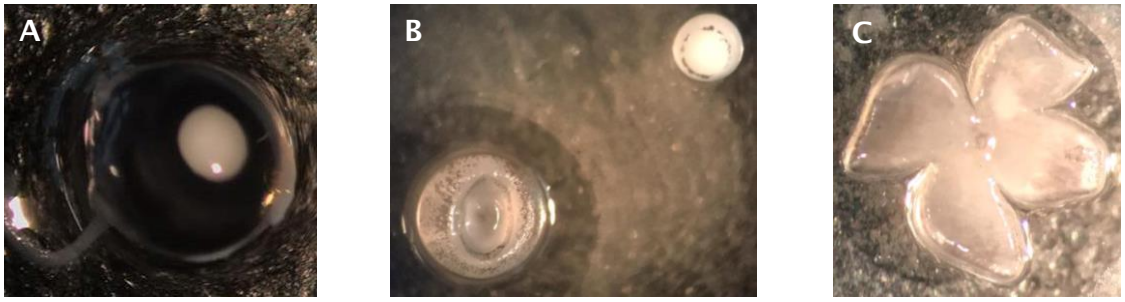

Figure 12 - Appearance of a neonatal retinal during dissection. (A) Eyeball without cornea. (B) Dissected eye without a lens marked by arrow. (C) Retina with four radial incisions. This image was taken using an iPhone camera through the lens of a stereoscope.

Retinas obtained at postnatal day (P)5 were whole mounted, stained with isolectin B4-Alexa 488 and imaged using a confocal microscope. A initial overview of the vascular organization of the retina was obtained at a low magnification (10x) (figure 13A and 13B). This was followed by a more detailed analysis of the vascular network using a higher magnification (20x) (figure 13C). The whole process of dissection, mounting and staining is technically difficult. This is illustrated in Figure 14, showing progressively improved representations of the retinal vascular network (poor, intermediate and good), that translate my learning curve. Red asterisks represent different types of damage that could be found in various areas of the retina. Figure 14G-14I represents some examples of the best retinal images obtained. Endothelial cells project filopodia at the tip of sprouting blood vessels as revealed in Figure 14I. In green, key retinal vascular measurements are depicted and in yellow some of the vascular components are shown. An example of the sprouting front is shown figure 13A.

Isolectin-B4-labelled endothelial cells were analyzed for key features of angiogenesis, such as vascular density (VD), vascular length (VL), and vascular outgrowth (VOg). Venules and arterioles could also be easily distinguished within the vascular network.

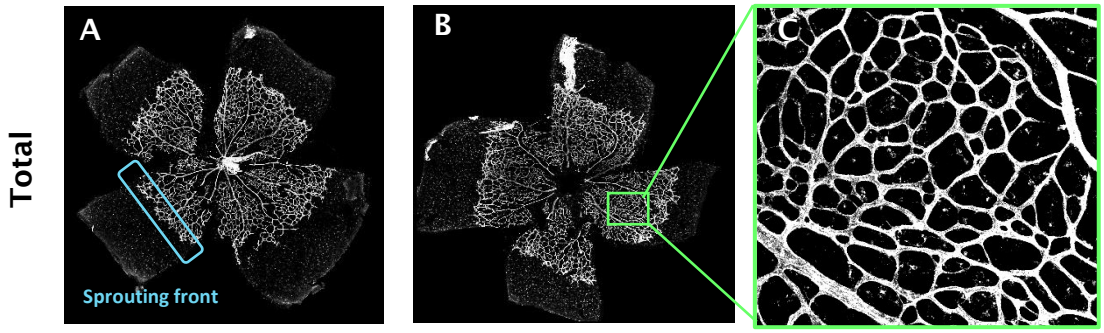

Figure 13 - Manipulation of retinal angiogenesis by immunofluorescence. (A) and (B) Retinal whole mount from postnatal day P5 were stained for endothelial cells with Isolectin B4-Alexa 594. An example of mouse vascular density is shown in (C).

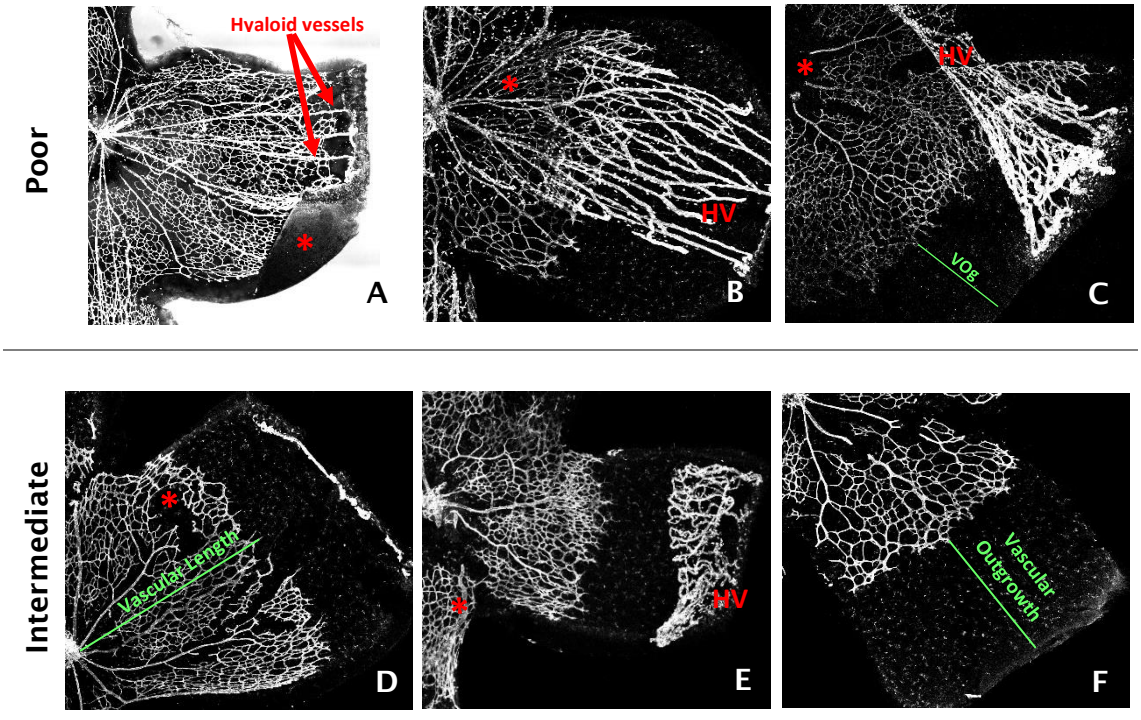

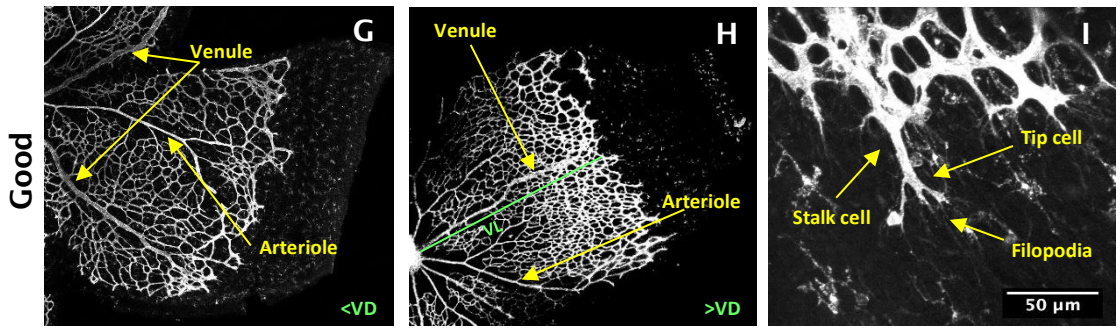

Figure 14 - Retina as a material for vascular cell biology. (A) (B) (C) (D) (E) (F) (G) (H) (I) – Magnified view of growing vascular edges in the P5 retina stained with isolectin-B4. Endothelial cells project numerous Filopodia at the tip of sprouting blood vessels. (I) – Sprouting front.

2.1. Assessment of the parameters of the developing vascular network

2.1.1. Evaluation of Vascular Length and Vascular Outgrowth (n biological)

I initially evaluated the vascular length (Figure 15A), which corresponds to the distance from the center to the tip of the vascular network for each condition (no treatment, tamoxifen, and tamoxifen plus iron) in $Nrf2^{flox}$ mice. I also evaluated the vascular outgrowth, which corresponds to the distance from filopodia to the edge of the retina (Figure 15B). In the comparisons here reported, each data point corresponded to the biological n (each data point is a mouse). As shown in figure 15A, in $Nrf2^{flox}$ mice, vascular lengths are similar for all conditions with no significant differences observed. The vascular length varied between 698.559-1255.043µm, 742.636-1170.158µm, and 948.088-1218.815µm in the no treatment, tamoxifen, and tamoxifen plus iron (T+I) groups, respectively. Regarding to vascular outgrowth, figure 15B shows that tamoxifen treatment did not lead to statically significant differences. However, tamoxifen plus iron was associated with a statistically significant increase in vascular outgrowth, when compared both to the no treatment and to the tamoxifen-only groups. The vascular outgrowth varied between 367.658-658.776µm, 509.727-825.003µm, and 663.880-929.880µm in no treatment, tamoxifen, and tamoxifen plus iron (T+I), respectively.

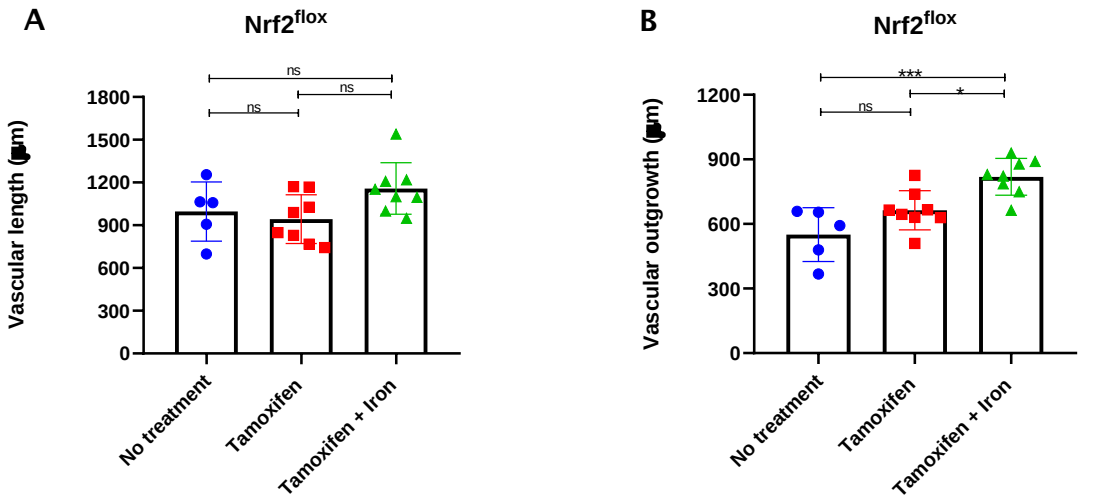

Figure 15 - Vascular length (A) and Vascular Outgrowth measured for each condition in $Nrf2^{flox}$ using a n biological. See in attachment, table 10 and 11 to observed in more detail the values obtained.

To understand the putative role of endothelial Nrf2 expression in the susceptibility of endothelial cells to iron *in vivo*, we also analyze for each animal, the role of iron in the vascular length and vascular outgrowth between $Nrf2^{flox}$ and $Nrf2^{i\Delta EC/+}$ as is shown in figure 16A and 16B. It should be highlighted that although the goal was initially to obtain Cdh5-CreER;$Nrf2^{lox/lox}$ homozygous newborns for analysis, this was unfortunately possible due to breeding and rederivation issues. Alternatively, I analyzed Cdh5-CreER;$Nrf2^{lox/+}$ heterozygous newborns ($Nrf2^{i\Delta EC/+}$), which have only 1 allele deleted and half of the gene dosage. I observed that decreased Nrf2 expression in $Nrf2^{i\Delta EC/+}$ mice were not associated with statistically significant differences in the vascular length or in the vascular outgrowth. The vascular length varied between 1095.595-1540.123µm and 939.236-1316.039µm in $Nrf2^{flox}$ and $Nrf2^{i\Delta EC/+}$, respectively. The vascular outgrowth varied between 663.880-890.974µm and 555.242-1066.512µm in $Nrf2^{flox}$ and $Nrf2^{i\Delta EC/+}$, respectively.

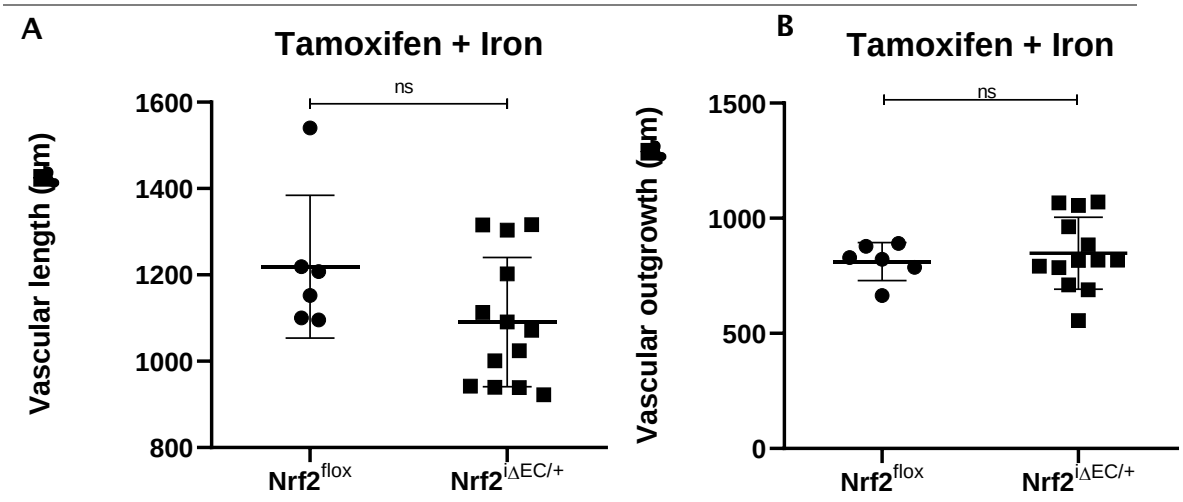

Figure 16 – Evaluation of vascular length (A) and vascular outgrowth (B) of endothelial-specific Nfr2 knock-out mice when exposed to iron. See in attachment, table 12 and 13 to observed in more detail the values obtained.

An example of a retina stained with isolectin-B4 for each type of treatment in $Nrf2^{flox}$ mice is presented in table 8 below:

Table 8 – Immunostaining of whole mount retina (P5) with Isolectin B4-Alexa488 (green) in $Nrf2^{flox}$ mice. Alternating pattern of arteries and veins.

No treatment	Tamoxifen	Tamoxifen + Iron
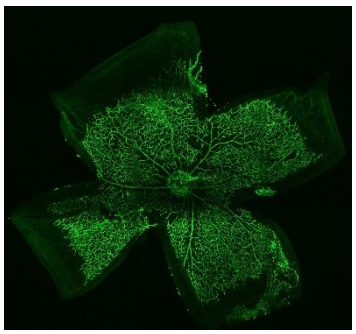	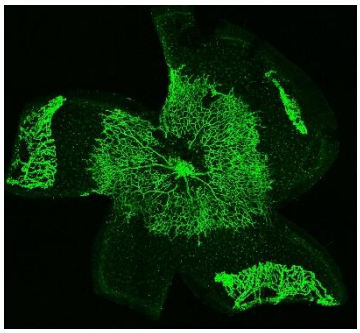	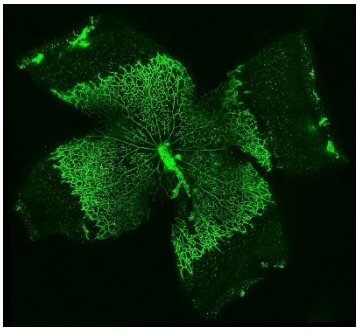

2.1.2. Evaluation of Vascular Length and Vascular Outgrowth (n measurements)

I also analyzed the vascular length (figure 17A) and vascular outgrowth (figure 17B) as described in 2.1.1 but taking into account all measurements (three measurements in each retina for each vascular parameter) for all treatment conditions (no treatment, tamoxifen, and tamoxifen plus iron) in $Nrf2^{flox}$ mice. Means were compared in groups and according to the results shown in figure 17A it is possible to verify that in $Nrf2^{flox}$ mice, vascular lengths are similar to each other, with no significant differences observed when comparing the groups that underwent some type of intraperitoneal treatment (tamoxifen or tamoxifen plus iron) with the group that had no treatment. However, there were statistically significant differences between the treated groups. The vascular length varied between 636.691-1377.284µm, 548.395-1236.374µm, and 757.896-1703.229µm in no treatment, tamoxifen, and tamoxifen plus iron (T+I), respectively. Regarding the vascular outgrowth, figure 17B shows that all groups have statistically significant differences between themselves. The vascular outgrowth varied between 211.17-773.918µm, 419.957-907.511µm, and 496.788-1071.466µm in no treatment, tamoxifen, and tamoxifen plus iron (T+I), respectively.

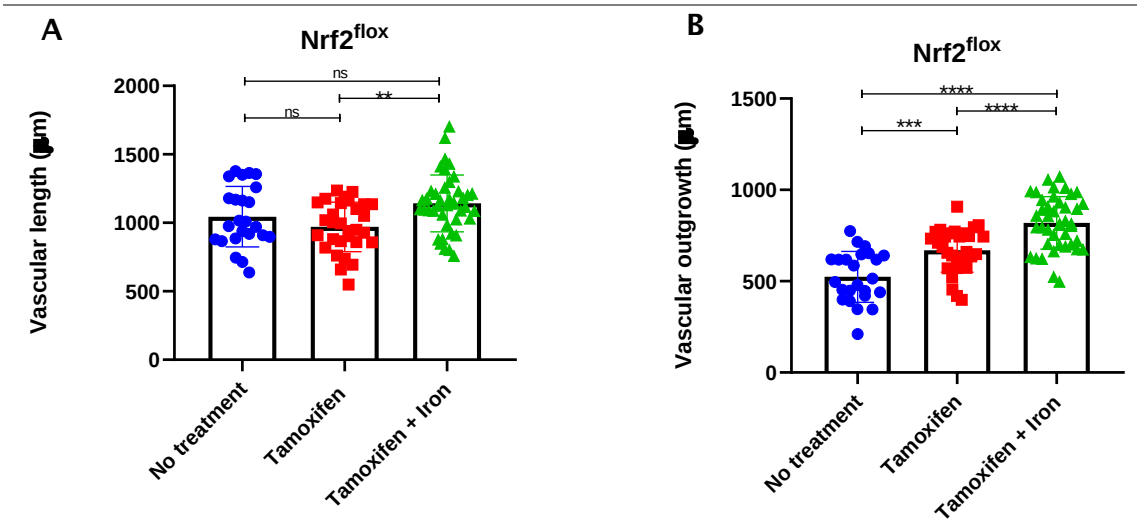

Figure 17 - Vascular length (A) and Vascular Outgrowth measured for each condition in $Nrf2^{flox}$ using a n measurement. See in attachment, table 14 and 15 to observed in more detail the values obtained.

Once again, to verify if Nrf2 contributes to the susceptibility of endothelial cells to iron *in vivo*, I also analyzed the role of iron in the vascular length and vascular outgrowth between $Nrf2^{flox}$ and $Nrf2^{i\Delta EC/+}$ as is shown in figure 18A and 18B. No statistically significant differences were found. The vascular length varied between 757.896-1703.229µm and 768.495-1588,052µm in $Nrf2^{flox}$ and $Nrf2^{i\Delta EC/+}$, respectively. The vascular outgrowth varied between 496.788-1055.393µm and 620.146-1237.683µm in $Nrf2^{flox}$ and $Nrf2^{i\Delta EC/+}$, respectively.

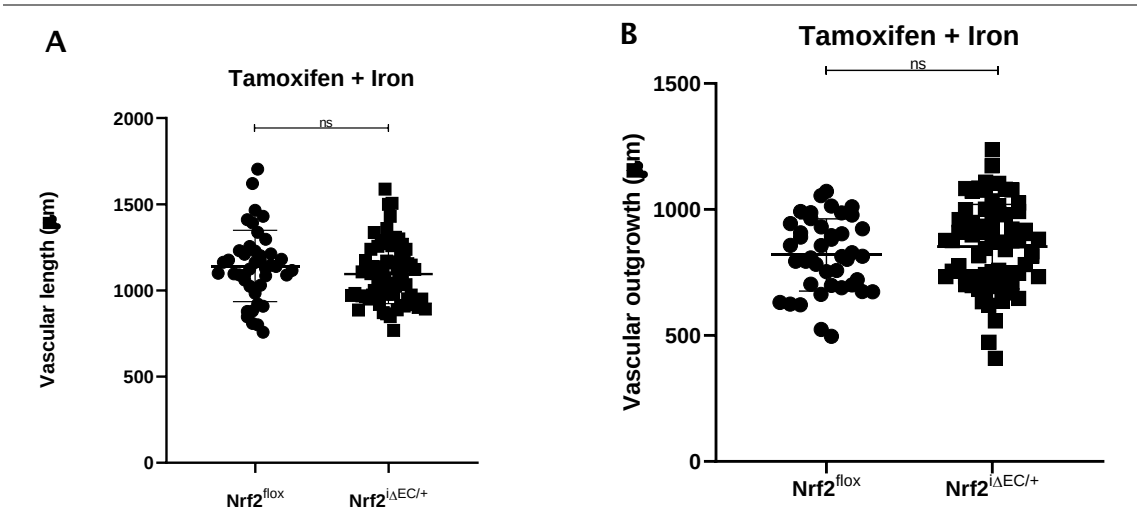

Figure 18 - Evaluation of vascular length (A) and vascular outgrowth (B) of endothelial-specific Nfr2 knock-out mice when exposed to iron. See in attachment, table 16 and 17 to observed in more detail the values obtained.

2.1.3. Ratio assessment (Vascular Length and Vascular Outgrowth)

Because iron treatment consistently led to increased vascular length and vascular outgrowth, I reasoned that iron could be stimulating tissue expansion and organism growth, affecting not only vasculature but also the retina size. Furthermore, I noticed that iron-treated pups were increased in relative size. To compensate for this potential effect, a new parameter was created - the ratio between vascular length and vascular outgrowth, as shown in figure 19. The graph display that regardless of the genotype and the treatment applied to the mice, the differences between all groups are not statistically significant and, therefore, the size of the pups does not influence the measurements of vascular length and vascular outgrowth made previously. The ratio varied between 0.515-

0.773, 0.482-0.668 and 0.505-0.645 in no treatment, tamoxifen, and tamoxifen plus iron group, respectively in Nrf2^{flox} pups, while in EC-specific KO the ratio varied between 0.463-0.703.

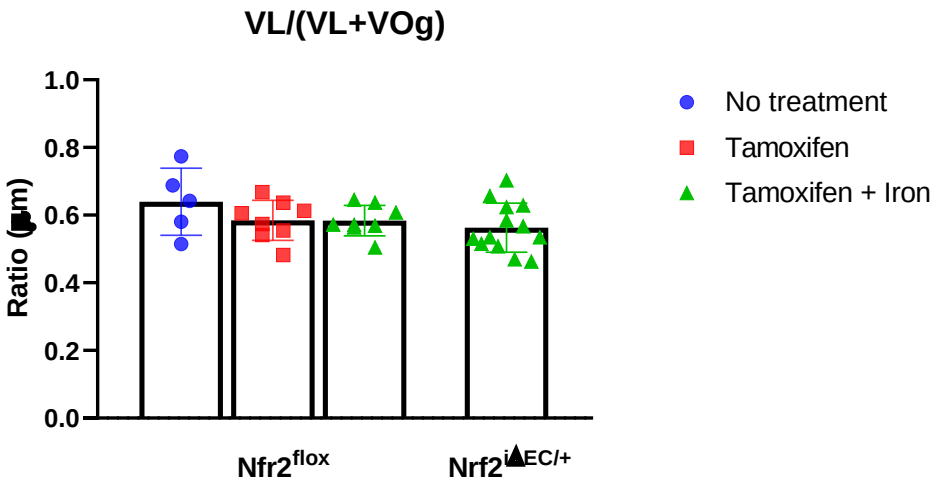

Figure 19 - Evaluation of differences in ratio VL/(VL+VOg) parameter in the Nrf2^{flox} and Nrf2$^{i\Delta EC/+}$ pup retina (P5). See in attachment, table 18, to observed in more detail the values obtained.

2.1.4. Assessment of the number of Veins and Arteries

Another vascular parameter that was evaluated was the vein/artery ratio present in the retinas, illustrated in figure 20.

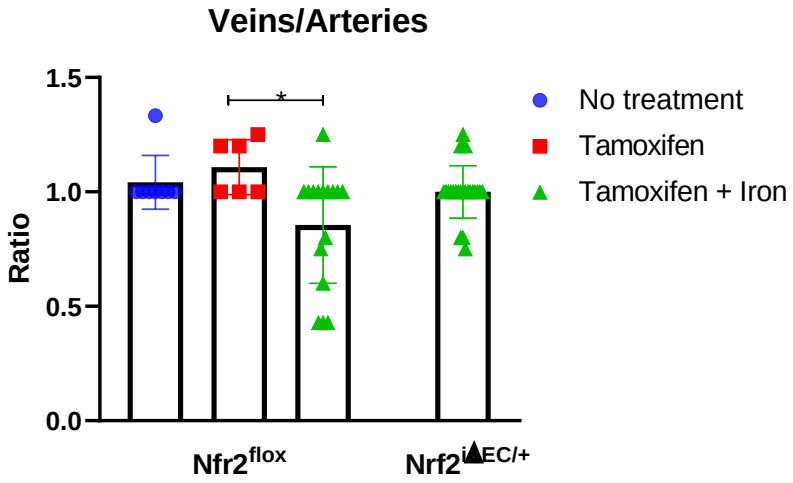

Figure 20 - Evaluation of differences in ratio between veins and arteries in the Nrf2^{flox} and Nrf2$^{i\Delta EC/+}$ pup retina (P5). See in attachment, table 19, to observed in more detail the values obtained.

No significant differences were observed between genotypes and type of treatment, with the exception for the difference between the group injected with tamoxifen and the group of Nrf2^{flox} pups that were injected with tamoxifen plus iron. Despite ratio variations between 1.00-1.33 in no treatment group, I found that all the ratio is always 1.00, except for the outlier value equal to 1.33. Besides that, the ratio varied between 1.00-1.25 and 0.43-1.25 in tamoxifen, and tamoxifen plus iron group, respectively, in Nrf2^{flox} pups, while in EC-specific KO the ratio varied between 0.75-1.25.

2.1.5. Assessment of the presence of Microhemorrhages

To study the permeability of the retinal vasculature endothelial cells, I performed a Ter-119 staining, to specifically label erythrocytes. A damaged retina was used as a positive control to confirm the labelling of extravasated erythrocytes (Figure 21A). In figure 21B, it is possible to confirm the presence of intravascular erythrocytes.

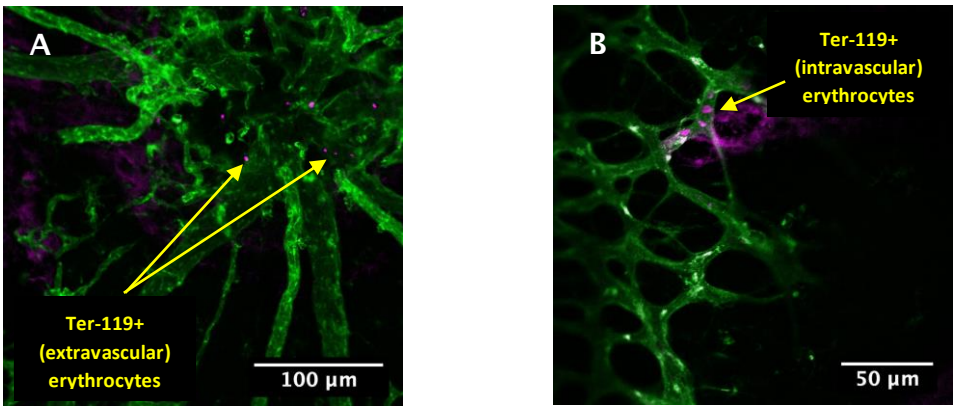

Figure 21 - Evaluation of the presence of microhemorrhages. (A extravascular erythrocytes and (B) intravascular erythrocytes.

I also evaluated the presence of microhemorrhages as a vascular parameter, illustrated in figure 22. According to the graph is possible to observe that when administrated tamoxifen plus iron on EC-specific KO, these mice display a higher number of hemorrhagic foci when compared to the control

group for all treatment conditions (no treatment, tamoxifen, tamoxifen plus iron). Despite the difference observed, this is not statistically significant.

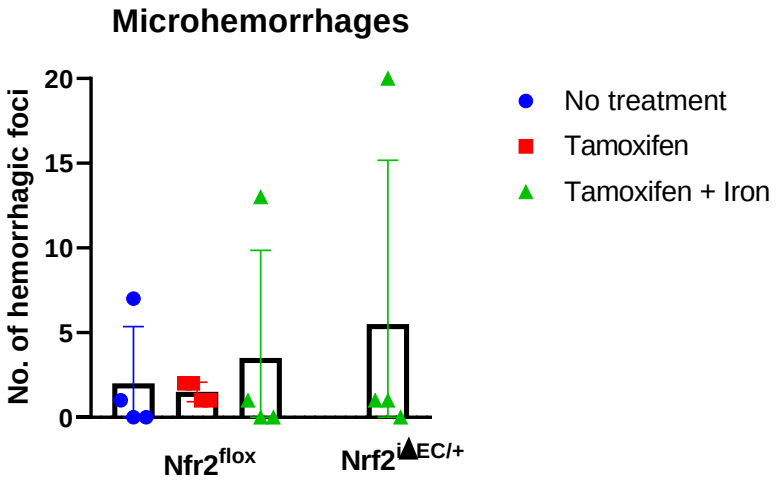

Figure 22 – Evaluation of number of hemorrhagic foci in each condition for $Nrf2^{flox}$ and $Nrf2^{i\Delta EC/+}$.

CHAPTER 4. DISCUSSION

Iron is a crucial element required for many biological processes in our body and its deficiency or excess (iron overload) is associated with disease.

Red blood cell transfusions are commonly used to treat severe anemia and, when repeated, may lead to secondary iron overload. AML is often associated with loss of non-malignant hematopoiesis and anemia, as a consequence of disease progression and chemotherapy. Recently, our group has shown that increased circulating iron levels are observed in AML at diagnosis, independently of the transfusional status. Interestingly, iron overload and increased ferritin levels in AML patients undergoing allogeneic hematopoietic stem cell transplantation have been associated with increased non-relapse mortality (caused by infection, or poor engraftment). One of the possible mechanisms underlying this association is the iron-induced damage of the bone marrow microenvironment, namely the vascular niche, which is fundamental for the support of HSCs and normal hematopoiesis. Our group has previously shown that AML-burdened mice treated with the iron chelator desferoxamine have recovered bone-lining endosteal vessels and improved HSC homing to the bone marrow[77]. This suggests that iron may be playing an important role in the local damage of the bone marrow vasculature. Therefore, we decided to study the putative toxic role of iron on endothelial cells using a simple *in vivo* model, the retinal angiogenesis model.

As a first step, we isolated plasma and bone marrow fluid (along with mononuclear cells) from AML patients in order to quantify ferritin and thus evaluate potential differences in iron storages between the two sites in AML. In the cytosol, iron is stored in ferritin. Ferritin plays a central role in modulating the amount of intracellular free iron and thus prevents the generation of iron-mediated oxidative stress[99]. Figure 11 shows the quantification of ferritin in our samples. All patients had higher values of ferritin in their bone marrow than in plasma, and the difference was statistically significant. Thus, it is concluded that the bone marrow is a more prone site for the storage of iron than plasma, and it is thus, verified once again the excess of iron present in leukemia patients. Ali et al., and Jacobs et al., demonstrate that the ferritin content of immature red cells in human bone marrow was found in higher concentrations than that found in peripheral mature red blood cells[109]. Additionally, ferritin is found only in BM smears and appeared to be largely confined to erythroid precursors and reticuloendothelial cells. On the other hand, in AML and myelodysplastic syndromes (MDS) with excess blasts, ferritin could be detected also in immature

myeloid cells[110]. Despite increasing evidence for iron overload and its toxicity, monitoring and management of secondary iron overload in patients with hematological malignancies as AML is still not common practice[111].

This present research project also aims to partially address a larger question that is being investigated in our group in a larger project: is the iron in the bone marrow important in the interaction between the stroma and leukemia cells? Previous results by Duarte et al., have shown that AML cells selectively destroy bone-lining endosteal blood vessels. Specifically, the number of endothelial cells is decreased, and vascular permeability is increased[77]. Huang et al., also suggest that iron overload impairs bone marrow mesenchymal stromal cells from higher-risk MDS patients by regulating the ROS-related Wnt/β-Catenin Pathway [112]. In this sense, in this experimental work we studied the in vivo effect of iron on endothelial cells, exploring, in detail, an alternative model study blood vessel – the retinal angiogenesis model - through the evaluation of various vascular parameters.

Although deferoxamine has been suggested as a molecule that helps in the preservation of the endosteal endothelium, thus rescuing the loss of HSCs, the mechanism underlying this vascular remodeling remains undiscovered[77]. Preliminary data show that endosteal endothelial cells do not correctly express heme oxygenase-1 (Hmox1), which is downstream of the master antioxidant transcription factor Nrf2. In this way, with the study of the role of iron in endothelial cells, we sought to evaluate the consequence of endothelial-specific deletion of Nrf2 in the vascular response to iron toxicity. Altogether, we aimed to use the well-described retinal angiogenesis model to study the *in vivo* iron-induced damage of endothelial cells and the putative role of Nrf2 in this process.

We were able to obtain images of stained whole mount preparations of neonatal mouse retina, a quantifiable and physiologically relevant model of angiogenesis. The eye, like any eye, is complex and is formed by different compartments and structures, among them, the retina.

Although the retina has been extensively used as a tool to study vascular biology, due to its multiple advantages already described, it is not always easy to perform some of the steps that the protocol requires. The small size of the mouse eye as well as its round shape (Figure 12A), require a lot of practice and precision during the dissection on stereoscope. After isolating the retina from the remaining components of the eye, the retina should look like a four-leaf clover (figure 12C). Even during the collecting of newborn's eye, it is necessary

to proceed with extra care so as not to crush the eye with the tweezers. The retina is an extremely fragile structure that must be handled with great care as mentioned above. According to the protocol described in Dr. Veronique Gebala PhD thesis, which we used as a guide, the eyes are collected and placed directly at 4% PFA and 3h later, 3 to 5 washes with PBS 1x are performed [113]. However, Tual-Chalot et al., have mentioned that dissection of eyes prepared in 2x concentration of PBS is important because this causes a small amount of water loss from the eye and reduces the intra-orbital pressure, which facilitates dissection and prolonged fixation time with PFA could lead to a high level of background and decreased resolution during retina analyzes.

Figure 14 depicts three types of retinas according to their vascular integrity – poor, intermediate, and good retinas. The “poor” quality retinas (figure 14A-C) have their vascular integrity compromised, and several possible reasons could explain it. First, the retinas may have been poorly dissected by one or more following reasons mentioned: the mounting of the retinas on a slide was not well achieved and as such, the edges of the retinas were bent (14A with an asterisk); they were accidentally torn away some part of their vasculature with the handling of tweezers (figure 14B and 14C with an asterisk); or hyaloid vessels were not well removed which after reduces the efficiently of the antibody staining, leading to high levels of background and decreased resolution when retinas were imaged on a confocal laser-scanning microscope. All these reasons mentioned complicate or prevent a reliable analysis of the target vascular parameters of the study in the respective damaged parts of the retina. Retinas with “intermediate” vascular integrity (figure 14D-F) present some of the complications mentioned above with less impact, such as the hyaloid vessels not well removed, rather than coinciding with the retinal vasculature, are only present at the edge of the retina (figure 14E) or the torn parts of the retina (figure 14D) likewise allow counting the number of venules and arterioles in the retina and measuring the vascular length. The "good" retinas (figure 14G-I) have no obstacles to the analysis of their vasculature, and easily allow the analysis of all the necessary parameters, including analysis of vascular density in any part of the vasculature. Figure 14G is an example of a retina with lower vascular density when compared to Figure 14H, since the latter shows a larger network of blood vessels. Moreover, when the vasculature network is not damaged, it is possible to verify that endothelial cells project filopodia at the tip of sprouting blood vessels.

After retina dissection, the next step in the procedure is immunofluorescence staining, which includes choosing the appropriate antibodies in the right concentration. In fact, exaggerated antibody concentrations can generate background in image analysis. Bright fluorescent spots may deposit in the tissue and impair the analysis of the blood vessels. These spots are precipitated aggregates of antibody and their formation may be prevented by removal through high-speed centrifugation of the antibody for (10,000 rpm for 5 min) before incubation. Two antibodies and one lectin were used to perform the immunostaining in this study. The primary antibody used was Biotin TER-119, a specific erythrocyte marker. The secondary antibody used was Streptavidin-PE, which binds to biotin TER119 and detects the presence of microhemorrhages (figure 21). Extravascular erythrocytes and intravascular erythrocytes are shown in figures 21A and 21B, respectively. TER-119 allowed studying the permeability of the retina's endothelial cells to answer the question of whether free iron, as observed in AML, induces an increase in vivo vascular permeability. According to the graph in figure 22, when administrated tamoxifen plus iron on EC-specific KO, mice display a higher number of hemorrhagic foci when compared to the control group for all treatment conditions (no treatment, tamoxifen, tamoxifen plus iron). Despite the difference observed, this is not statistically significant. The lectin incorporated in the immunostaining, was Griffonia simplicifolia Isolectin B4 Alexa Fluor 488. Lectins are specific carbohydrate-binding proteins of nonimmune origin [114]. Among the larger family of lectins, GS-IB_4, has been shown a great tool for analysis of microvascular structure and function. In this case, Isolectin-B4 was used to label the endothelium. It is also important to say that Isolectin-B4 when purchased should be stored at -20° and as such, working aliquots should be made and kept at 4° to avoid repeated cycles of freeze thawing.

Once all the experimental work was carried out, the results obtained were analyzed in Image J and GraphPad. For this, it was necessary to perform genotyping of the mice previously in the I3S genotyping department. From this analysis, two genotypes were found: $Nrf2^{flox}$ and $Nrf2^{i\Delta EC/+}$. $Nrf2^{flox}$ was used as a control in this experience. It should be highlighted that the central question regarding the role of endothelial Nrf2 in response to iron was only partially addressed in the current project. Due to technical limitations as breeding and rederivation issues, and disruptions caused by the COVID-19 pandemic, endothelial-specific homozygous Nrf2 knockouts were not analyzed (Cdh5-

CreER;Nrf2lox/lox), as was initially pretended. Despite several attempts to obtain the desired genotype, only in the last litter was possible to obtain a mouse with the desired genotype. Since no conclusions can be inferred with an n=1, this mouse was excluded from the analysis. Thus, as an alternative Cdh5-CreER;Nrf2lox/+ mice were used to infer conclusions about the putative role of Nrf2 in mediating the susceptibility of endothelial cells to iron in vivo.

Due to its postnatal development and easy accessibility, the mouse retinal vasculature is an excellent model to study growth and remodeling during development and disease. Most studies only focus on a descriptive analysis of the model, and as such, this project comes to fills the lack of information on comparable quantitative measurements. In this sense, the following relevant vascular parameters were studied: vascular length, vascular outgrowth, vascular density, vein/arteries ratio, and the presence of microhemorrhages.

Regarding to vascular length and vascular outgrowth based on biological number mice, it was observed that vascular lengths (figure 15A) in all mice are similar for all conditions (no treatment, tamoxifen, and tamoxifen plus iron) and as such, there is no statistically significant differences observed in $Nrf2^{flox}$ mice, which means that here Nrf2 did not induce vascular growth. Similarly, analyzing vascular outgrowth (figure 15B) it is possible observe that tamoxifen treatment did not lead to statically significant differences. However, when analyzed tamoxifen plus iron was associated with a statistically significant increase in vascular outgrowth, when compared both to the no treatment and to the tamoxifen-only groups. Thus, we can suggest that iron promotes retinal size growth. In order to understand the putative role of endothelial Nrf2 expression in the susceptibility of endothelial cells to iron *in vivo*, it was evaluated the vascular length and vascular outgrowth in $Nrf2^{flox}$ and in EC-specific KO mice, $Nrf2^{i\Delta EC/+}$ (figure 16). Here, I have observed that mice with the partially deleted Nrf2 gene do not display statistically significant differences with the control group either in vascular length or in vascular outgrowth and as such, it can be suggested that the partially deleted Nrf2 does not mediate susceptibility in iron-induced endothelial cells. After it was performed an analysis in more detail, using three measures of vascular length and vascular outgrowth in each retina, instead of using the biological number (figure 17). Using all measurements, significant statistical differences arise for the vascular outgrowth parameter in tamoxifen, and tamoxifen plus iron regarding the no treatment group (figure 17B). Differences in vascular length also appeared in the tamoxifen plus iron

group compared to mice that were not exposed to any type of treatment. Once again, iron seems to have some influence on the permeability of endothelial cells. Again, with the purpose of evaluating the role of nrf2 in this process, I evaluated the condition of treatment with tamoxifen and iron dextran in both genotypes (figure 18). As shown in results obtained in figure 16 using a biological n as a measurement, even using the three measurements on each retina of each animal, no statistically significant differences are still found. Thus, despite Nrf2 being related with Hmox1, which is an essential enzyme to iron catabolism, and which is not correctly express by endosteal endothelial cells did not correctly express, Nrf2 seems not have an important role in susceptibility induced apparently by iron in vivo. The following vascular parameter evaluated was a ratio performed between vascular length and vascular outgrowth which was created to correct the eventually difference in size that pups have, in order to make the analysis previously done more viable. According to the figure 19, there is no differences between all treatments in both genotypes, $Nrf2^{flox}$ and $Nrf2^{i\Delta EC/+}$, which means the size of the pups does not influence the measurements of vascular length and vascular outgrowth made previously. Thus, this result suggests that all differences previously verified, have therefore some role of the iron involved. Table 8 shows three retinas stained with Isolectin-B4 with no treatment, tamoxifen injection and tamoxifen plus iron injection, respectively. Morphologically, the retinas appear to be similar.

Despite the question “Is Nrf2 mediating the susceptibility of endothelial cells to iron in vivo?” has never been answered by none study previously performed by other research groups, Nrf2 has been mentioned as promotor of several oncogenes unrelated to the antioxidant activity, as Vascular endothelial growth factor A (VEGF-A)[115]. A review has also summarized the the mechanisms that regulate the Nrf2/Keap1-ARE signaling pathway and the latest advances in understanding how Nrf2 protects against oxidative stress-induced endothelial injuries [116]. Besides that, Lim et al., have reported that Nrf2 is activated by iron-induced, mitochondria-derived pro-oxidants and drives Bmp6 expression in liver sinusoid endothelial cells, which in turn increases hepcidin synthesis by neighbouring hepatocytes. They have also proposed that Nrf2 links cellular sensing of excess toxic iron to control of systemic iron homeostasis and antioxidant responses[117]. Thus, Nrf2 could be considered as therapeutic target for iron-associated disorders, including AML.

CHAPTER 4. CONCLUSION

The establishment of the retinal angiogenesis model required significant technical training and practice. The entire process of dissection, immunofluorescence and retinal assembly is sensitive to small mistakes that may compromise the quality of the final analysis of the vasculature.

Although we have obtained in general negative results to the initial hypothesized question and to what was initially expected, we can conclude that the aim to use the well-described retinal angiogenesis model to study the *in vivo* iron-induced damage of endothelial cells was fulfilled. It should be highlighted that the central question regarding the role of endothelial Nrf2 in response to iron was only partially addressed in the current project. Due to technical limitations and disruptions caused by the COVID-19 pandemic, only endothelial-specific heterozygous Nrf2 knockouts (Cdh5-CreER;$Nrf2^{lox/+}$) were generated and those mice did not show particular vascular defects, decreased angiogenesis or increased vascular permeability in response to iron dextran administration. However, the partial expression of Nrf2 in endothelial cells from Cdh5-CreER;$Nrf2^{lox/+}$ may be sufficient to adequately respond to iron toxicity.

Future work should repeat a similar workflow and analysis using Cdh5-CreER;$Nrf2^{lox/lox}$, which have total loss of Nrf2 expression in endothelial cells.

This project had implications in understanding the mechanisms driving the remodeling of the vascular niche in acute myeloid leukemia and in demonstrating the role of endothelial Nrf2 antioxidant responses.

BIBLIOGRAPHIC REFERENCES

1. Ma, X. and H. Yu, Global burden of cancer. Yale J Biol Med, 2006. **79**(3-4): p. 85-94.
2. Passegué, E., et al., Normal and leukemic hematopoiesis: are leukemias a stem cell disorder or a reacquisition of stem cell characteristics? Proc Natl Acad Sci U S A, 2003. **100 Suppl 1**(Suppl 1): p. 11842-9.
3. Schlenk, R.F., Post-remission therapy for acute myeloid leukemia. Haematologica, 2014. **99**(11): p. 1663-1670.
4. Döhner, H., D.J. Weisdorf, and C.D. Bloomfield, Acute Myeloid Leukemia. N Engl J Med, 2015. **373**(12): p. 1136-52.
5. Parkin DM, W.S., Ferlay J, Teppo L, Thomas DB, Cancer Incidence in Five Continents. **III**.
6. Ferlay, J., et al., Cancer Incidence, Mortality and Prevalence Worldwide, version 1.0, Lyon: International Agency for Research on Cancer. IARC Cancer Base no, 2000. **1**.
7. Orazi, E.J.D.A.E.C.L.Q.-M.A., Hematopathology ed. n. Edition. 27th June 2016.
8. Pelcovits, A. and R. Niroula, Acute Myeloid Leukemia: A Review. R I Med J (2013), 2020. **103**(3): p. 38-40.
9. Saultz, J.N. and R. Garzon, Acute Myeloid Leukemia: A Concise Review. J Clin Med, 2016. **5**(3).
10. Campos, L., et al., Surface marker expression in adult acute myeloid leukaemia: correlations with initial characteristics, morphology and response to therapy. Br J Haematol, 1989. **72**(2): p. 161-6.
11. Kumar, C.C., Genetic abnormalities and challenges in the treatment of acute myeloid leukemia. Genes & cancer, 2011. **2**(2): p. 95-107.
12. Arber, D.A., et al., The 2016 revision to the World Health Organization classification of myeloid neoplasms and acute leukemia. Blood, 2016. **127**(20): p. 2391-405.
13. Song, X., et al., Incidence, Survival, and Risk Factors for Adults with Acute Myeloid Leukemia Not Otherwise Specified and Acute Myeloid Leukemia with Recurrent Genetic Abnormalities: Analysis of the Surveillance, Epidemiology, and End Results (SEER) Database, 2001-2013. Acta Haematol, 2018. **139**(2): p. 115-127.

14. Byrd, J.C., et al., Pretreatment cytogenetic abnormalities are predictive of induction success, cumulative incidence of relapse, and overall survival in adult patients with de novo acute myeloid leukemia: results from Cancer and Leukemia Group B (CALGB 8461). Blood, 2002. **100**(13): p. 4325-36.
15. Döhner, H., et al., Diagnosis and management of AML in adults: 2017 ELN recommendations from an international expert panel. Blood, 2017. **129**(4): p. 424-447.
16. Döhner, H., et al., Diagnosis and management of acute myeloid leukemia in adults: recommendations from an international expert panel, on behalf of the European LeukemiaNet. Blood, 2010. **115**(3): p. 453-74.
17. Dohner, K., et al., Mutant nucleophosmin (NPM1) predicts favorable prognosis in younger adults with acute myeloid leukemia and normal cytogenetics: interaction with other gene mutations. Blood, 2005. **106**(12): p. 3740-3746.
18. Smith, M., et al., Adult acute myeloid leukaemia. Crit Rev Oncol Hematol, 2004. **50**(3): p. 197-222.
19. Döhner, H., D.J. Weisdorf, and C.D. Bloomfield, Acute Myeloid Leukemia. New England Journal of Medicine, 2015. **373**(12): p. 1136-1152.
20. Othus, M., et al., Complete Remissions (CRs) with Azacitidine Regimens Compared to Crs with 7+3 Induction Chemotherapy and the Effect on Overall Survival. Blood, 2016. **128**(22): p. 1613.
21. Dombret, H. and C. Gardin, An update of current treatments for adult acute myeloid leukemia. Blood, 2016. **127**(1): p. 53-61.
22. Cassileth, P.A., et al., Varying intensity of postremission therapy in acute myeloid leukemia. Blood, 1992. **79**(8): p. 1924-30.
23. Wei, A.H. and I.S. Tiong, Midostaurin, enasidenib, CPX-351, gemtuzumab ozogamicin, and venetoclax bring new hope to AML. Blood, 2017. **130**(23): p. 2469-2474.
24. Szotkowski, T., et al., Secondary acute myeloid leukemia - a single center experience. Neoplasma, 2010. **57**(2): p. 170-8.
25. Leone, G., et al., Therapy-related leukemia and myelodysplasia: susceptibility and incidence. Haematologica, 2007. **92**(10): p. 1389-98.
26. Larson, R.A., Etiology and management of therapy-related myeloid leukemia. Hematology Am Soc Hematol Educ Program, 2007: p. 453-9.

27. Kayser, S., et al., The impact of therapy-related acute myeloid leukemia (AML) on outcome in 2853 adult patients with newly diagnosed AML. Blood, 2011. **117**(7): p. 2137-45.
28. Schoch, C., et al., Acute myeloid leukemia with a complex aberrant karyotype is a distinct biological entity characterized by genomic imbalances and a specific gene expression profile. Genes Chromosomes Cancer, 2005. **43**(3): p. 227-38.
29. Ok, C.Y., et al., Mutational profiling of therapy-related myelodysplastic syndromes and acute myeloid leukemia by next generation sequencing, a comparison with de novo diseases. Leuk Res, 2015. **39**(3): p. 348-54.
30. Pedersen-Bjergaard, J., et al., Genetics of therapy-related myelodysplasia and acute myeloid leukemia. Leukemia, 2008. **22**(2): p. 240-8.
31. Hall, A.P., The role of angiogenesis in cancer. Comparative Clinical Pathology, 2005. **13**(3): p. 95-99.
32. Burri, P.H., R. Hlushchuk, and V. Djonov, Intussusceptive angiogenesis: its emergence, its characteristics, and its significance. Dev Dyn, 2004. **231**(3): p. 474-88.
33. Gerhardt, H., et al., VEGF guides angiogenic sprouting utilizing endothelial tip cell filopodia. J Cell Biol, 2003. **161**(6): p. 1163-77.
34. Potente, M., H. Gerhardt, and P. Carmeliet, Basic and therapeutic aspects of angiogenesis. Cell, 2011. **146**(6): p. 873-87.
35. Haouas, H., Angiogenesis and acute myeloid leukemia. Hematology, 2014. **19**(6): p. 311-23.
36. Carmeliet, P. and R.K. Jain, Angiogenesis in cancer and other diseases. Nature, 2000. **407**(6801): p. 249-57.
37. Aguayo, A., et al., Angiogenesis in acute and chronic leukemias and myelodysplastic syndromes. Blood, 2000. **96**(6): p. 2240-5.
38. Folkman, J., Angiogenesis in cancer, vascular, rheumatoid and other disease. Nat Med, 1995. **1**(1): p. 27-31.
39. Litwin, C., et al., Role of the microenvironment in promoting angiogenesis in acute myeloid leukemia. Am J Hematol, 2002. **70**(1): p. 22-30.
40. Hussong, J.W., G.M. Rodgers, and P.J. Shami, Evidence of increased angiogenesis in patients with acute myeloid leukemia. Blood, 2000. **95**(1): p. 309-13.
41. Padró, T., et al., Increased angiogenesis in the bone marrow of patients with acute myeloid leukemia. Blood, 2000. **95**(8): p. 2637-44.

42. Kini, A.R., N.E. Kay, and L.C. Peterson, Increased bone marrow angiogenesis in B cell chronic lymphocytic leukemia. Leukemia, 2000. **14**(8): p. 1414-8.
43. Hicklin, D.J. and L.M. Ellis, Role of the vascular endothelial growth factor pathway in tumor growth and angiogenesis. J Clin Oncol, 2005. **23**(5): p. 1011-27.
44. Padró, T., et al., Overexpression of vascular endothelial growth factor (VEGF) and its cellular receptor KDR (VEGFR-2) in the bone marrow of patients with acute myeloid leukemia. Leukemia, 2002. **16**(7): p. 1302-10.
45. Andersen, M.L. and L.M.F. Winter, Animal models in biological and biomedical research - experimental and ethical concerns. An Acad Bras Cienc, 2019. **91**(suppl 1): p. e20170238.
46. Stahl, A., et al., The mouse retina as an angiogenesis model. Investigative ophthalmology & visual science, 2010. **51**(6): p. 2813-2826.
47. Alon, T., et al., Vascular endothelial growth factor acts as a survival factor for newly formed retinal vessels and has implications for retinopathy of prematurity. Nat Med, 1995. **1**(10): p. 1024-8.
48. Stalmans, I., et al., Arteriolar and venular patterning in retinas of mice selectively expressing VEGF isoforms. The Journal of clinical investigation, 2002. **109**(3): p. 327-336.
49. Dorrell, M.I., et al., Adult bone marrow-derived stem cells use R-cadherin to target sites of neovascularization in the developing retina. Blood, 2004. **103**(9): p. 3420-7.
50. Otani, A., et al., Rescue of retinal degeneration by intravitreally injected adult bone marrow-derived lineage-negative hematopoietic stem cells. J Clin Invest, 2004. **114**(6): p. 765-74.
51. Otani, A., et al., Bone marrow-derived stem cells target retinal astrocytes and can promote or inhibit retinal angiogenesis. Nat Med, 2002. **8**(9): p. 1004-10.
52. Benedito, R., et al., The notch ligands Dll4 and Jagged1 have opposing effects on angiogenesis. Cell, 2009. **137**(6): p. 1124-35.
53. Pitulescu, M.E., et al., Inducible gene targeting in the neonatal vasculature and analysis of retinal angiogenesis in mice. Nature Protocols, 2010. **5**(9): p. 1518-1534.

54. Uemura, A., et al., Angiogenesis in the mouse retina: a model system for experimental manipulation. Exp Cell Res, 2006. **312**(5): p. 676-83.
55. Dorrell, M.I., et al., Combination angiostatic therapy completely inhibits ocular and tumor angiogenesis. Proc Natl Acad Sci U S A, 2007. **104**(3): p. 967-72.
56. Rennel, E.S., S.J. Harper, and D.O. Bates, Therapeutic potential of manipulating VEGF splice isoforms in oncology. Future Oncol, 2009. **5**(5): p. 703-12.
57. Brenner, M. and A. Messing, GFAP Transgenic Mice. Methods, 1996. **10**(3): p. 351-64.
58. Saint-Geniez, M. and P.A. D'Amore, Development and pathology of the hyaloid, choroidal and retinal vasculature. Int J Dev Biol, 2004. **48**(8-9): p. 1045-58.
59. Carmeliet, P. and R.K. Jain, Molecular mechanisms and clinical applications of angiogenesis. Nature, 2011. **473**(7347): p. 298-307.
60. Schnitzer, J., Astrocytes in the guinea pig, horse, and monkey retina: their occurrence coincides with the presence of blood vessels. Glia, 1988. **1**(1): p. 74-89.
61. Walter, T., et al., Visualization of image data from cells to organisms. Nat Methods, 2010. **7**(3 Suppl): p. S26-41.
62. Beard, J.L., Iron biology in immune function, muscle metabolism and neuronal functioning. J Nutr, 2001. **131**(2s-2): p. 568S-579S; discussion 580S.
63. Camaschella, C., Iron and hepcidin: a story of recycling and balance. Hematology Am Soc Hematol Educ Program, 2013. **2013**: p. 1-8.
64. Ganz, T., Systemic iron homeostasis. Physiol Rev, 2013. **93**(4): p. 1721-41.
65. Muckenthaler, M.U., et al., A Red Carpet for Iron Metabolism. Cell, 2017. **168**(3): p. 344-361.
66. Young, I., et al., Association between Haem and Non-Haem Iron Intake and Serum Ferritin in Healthy Young Women. Nutrients, 2018. **10**(1): p. 81.
67. Fairweather-Tait, S.J., Iron nutrition in the UK: getting the balance right. Proc Nutr Soc, 2004. **63**(4): p. 519-28.
68. Humans;, I.P.a.P.i., ron Physiology and Pathophysiology in Humans. Springer, 2012.

69. Gnana-Prakasam, J.P., et al., Expression and function of iron-regulatory proteins in retina. IUBMB Life, 2010. **62**(5): p. 363-70.
70. Camaschella, C., Iron-deficiency anemia. N Engl J Med, 2015. **372**(19): p. 1832-43.
71. Pantopoulos, K., et al., Mechanisms of mammalian iron homeostasis. Biochemistry, 2012. **51**(29): p. 5705-24.
72. Anderson, G.J., Mechanisms of iron loading and toxicity. Am J Hematol, 2007. **82**(12 Suppl): p. 1128-31.
73. Knovich, M.A., et al., Ferritin for the clinician. Blood reviews, 2009. **23**(3): p. 95-104.
74. Ryter, S.W., J. Alam, and A.M. Choi, Heme oxygenase-1/carbon monoxide: from basic science to therapeutic applications. Physiol Rev, 2006. **86**(2): p. 583-650.
75. Jung, M., et al., Iron as a Central Player and Promising Target in Cancer Progression. Int J Mol Sci, 2019. **20**(2).
76. Adamson, J.W., The relationship of erythropoietin and iron metabolism to red blood cell production in humans. Semin Oncol, 1994. **21**(2 Suppl 3): p. 9-15.
77. Duarte, D., et al., Inhibition of Endosteal Vascular Niche Remodeling Rescues Hematopoietic Stem Cell Loss in AML. Cell Stem Cell, 2018. **22**(1): p. 64-77.e6.
78. Callens, C., et al., Targeting iron homeostasis induces cellular differentiation and synergizes with differentiating agents in acute myeloid leukemia. J Exp Med, 2010. **207**(4): p. 731-50.
79. Stockwell, B.R., et al., Ferroptosis: A Regulated Cell Death Nexus Linking Metabolism, Redox Biology, and Disease. Cell, 2017. **171**(2): p. 273-285.
80. Du, Y., et al., Targeting ferroptosis contributes to ATPR-induced AML differentiation via ROS-autophagy-lysosomal pathway. Gene, 2020. **755**: p. 144889.
81. Lopes, M., et al., Loss of erythroblasts in acute myeloid leukemia causes iron redistribution with clinical implications. bioRxiv, 2020: p. 2020.10.26.350116.
82. Delavigne, K., et al., Hemophagocytic syndrome in patients with acute myeloid leukemia undergoing intensive chemotherapy. Haematologica, 2014. **99**(3): p. 474-80.

83. Gasparetto, M., et al., Low ferroportin expression in AML is correlated with good risk cytogenetics, improved outcomes and increased sensitivity to chemotherapy. Leuk Res, 2019. **80**: p. 1-10.
84. Remacha, Á.F., et al., Evolution of iron overload in patients with low-risk myelodysplastic syndrome: iron chelation therapy and organ complications. Annals of Hematology, 2015. **94**(5): p. 779-787.
85. Wang, W., et al., Serum ferritin: Past, present and future. Biochim Biophys Acta, 2010. **1800**(8): p. 760-9.
86. Ihlow, J., et al., AML: high serum ferritin at initial diagnosis has a negative impact on long-term survival. Leuk Lymphoma, 2019. **60**(1): p. 69-77.
87. Bertoli, S., et al., Ferritin heavy/light chain (FTH1/FTL) expression, serum ferritin levels, and their functional as well as prognostic roles in acute myeloid leukemia. Eur J Haematol, 2019. **102**(2): p. 131-142.
88. Tachibana, T., et al., Clinical Significance of Serum Ferritin at Diagnosis in Patients With Acute Myeloid Leukemia: A YACHT Multicenter Retrospective Study. Clin Lymphoma Myeloma Leuk, 2018. **18**(6): p. 415-421.
89. Lebon, D., et al., Hyperferritinemia at diagnosis predicts relapse and overall survival in younger AML patients with intermediate-risk cytogenetics. Leuk Res, 2015. **39**(8): p. 818-21.
90. Alkhateeb, A.A. and J.R. Connor, The significance of ferritin in cancer: Anti-oxidation, inflammation and tumorigenesis. Biochimica et Biophysica Acta (BBA) - Reviews on Cancer, 2013. **1836**(2): p. 245-254.
91. de Jong, P.T.V.M., A Historical Analysis of the Quest for the Origins of Aging Macula Disorder, the Tissues Involved, and Its Terminology. Ophthalmology and eye diseases, 2016. **8**(Suppl 1): p. 5-14.
92. Zhao, L., et al., A high serum iron level causes mouse retinal iron accumulation despite an intact blood-retinal barrier. Am J Pathol, 2014. **184**(11): p. 2862-7.
93. Moos, T., et al., Developmental iron uptake and axonal transport in the retina of the rat. Molecular and Cellular Neuroscience, 2011. **46**(3): p. 607-613.
94. Sajadimajd, S. and M. Khazaei, Oxidative Stress and Cancer: The Role of Nrf2. Curr Cancer Drug Targets, 2018. **18**(6): p. 538-557.

95. Valko, M., et al., Free radicals and antioxidants in normal physiological functions and human disease. Int J Biochem Cell Biol, 2007. **39**(1): p. 44-84.
96. Itoh, K., et al., Regulatory mechanisms of cellular response to oxidative stress. Free Radical Research, 1999. **31**(4): p. 319-324.
97. Yun, J., et al., Redox-dependent mechanisms in coronary collateral growth: the "redox window" hypothesis. Antioxidants & redox signaling, 2009. **11**(8): p. 1961-1974.
98. Finkel, T. and N.J. Holbrook, Oxidants, oxidative stress and the biology of ageing. Nature, 2000. **408**(6809): p. 239-47.
99. Altamura, S., et al., Regulation of iron homeostasis: Lessons from mouse models. Mol Aspects Med, 2020. **75**: p. 100872.
100. Milkovic, L., N. Zarkovic, and L. Saso, Controversy about pharmacological modulation of Nrf2 for cancer therapy. Redox Biol, 2017. **12**: p. 727-732.
101. Sporn, M.B. and K.T. Liby, NRF2 and cancer: the good, the bad and the importance of context. Nat Rev Cancer, 2012. **12**(8): p. 564-71.
102. Araujo, J.A., M. Zhang, and F. Yin, Heme oxygenase-1, oxidation, inflammation, and atherosclerosis. Front Pharmacol, 2012. **3**: p. 119.
103. Karathedath, S., et al., Role of NF-E2 related factor 2 (Nrf2) on chemotherapy resistance in acute myeloid leukemia (AML) and the effect of pharmacological inhibition of Nrf2. PLoS One, 2017. **12**(5): p. e0177227.
104. Grievink, H.W., et al., Comparison of Three Isolation Techniques for Human Peripheral Blood Mononuclear Cells: Cell Recovery and Viability, Population Composition, and Cell Functionality. Biopreserv Biobank, 2016. **14**(5): p. 410-415.
105. O'Neil, K.T., R.H. Hoess, and W.F. DeGrado, Design of DNA-binding peptides based on the leucine zipper motif. Science, 1990. **249**(4970): p. 774-8.
106. Sauer, B. and N. Henderson, Site-specific DNA recombination in mammalian cells by the Cre recombinase of bacteriophage P1. Proceedings of the National Academy of Sciences of the United States of America, 1988. **85**(14): p. 5166-5170.
107. Odell, I.D. and D. Cook, Immunofluorescence techniques. J Invest Dermatol, 2013. **133**(1): p. e4.

108. Arribas, S.M., et al., Imaging the vascular wall using confocal microscopy. The Journal of physiology, 2007. **584**(Pt 1): p. 5-9.
109. Ali, F.M., et al., Enrichment of erythroblasts from human bone marrow using complement-mediated lysis: measurement of ferritin. Br J Haematol, 1983. **53**(2): p. 227-35.
110. Invernizzi, R., et al., Immunocytochemical detection of ferritin in human bone marrow and peripheral blood cells using monoclonal antibodies specific for the H and L subunit. Br J Haematol, 1990. **76**(3): p. 427-32.
111. Remacha, A.F., et al., Iron overload and chelation therapy in patients with low-risk myelodysplastic syndromes with transfusion requirements. Ann Hematol, 2010. **89**(2): p. 147-54.
112. Huang, L., et al., Iron Overload Impairs Bone Marrow Mesenchymal Stromal Cells from Higher-Risk MDS Patients by Regulating the ROS-Related Wnt/β-Catenin Pathway. Stem Cells International, 2020. **2020**: p. 8855038.
113. Gebala, V.M., Mechanisms of lumen formation during sprouting angiogenesis in vivo. University College London and Cancer Research UK London Research Institute.
114. Benton, R.L., et al., Griffonia simplicifolia isolectin B4 identifies a specific subpopulation of angiogenic blood vessels following contusive spinal cord injury in the adult mouse. J Comp Neurol, 2008. **507**(1): p. 1031-52.
115. Zimta, A.A., et al., The Role of Nrf2 Activity in Cancer Development and Progression. Cancers (Basel), 2019. **11**(11).
116. Chen, B., et al., The role of Nrf2 in oxidative stress-induced endothelial injuries. J Endocrinol, 2015. **225**(3): p. R83-99.
117. Lim, P.J., et al., Nrf2 controls iron homeostasis in haemochromatosis and thalassaemia via Bmp6 and hepcidin. Nat Metab, 2019. **1**(5): p. 519-531.

ATTACHEMENTS

- FERRITIN ASSAY

Table 9 – Ferritin values in human plasm and bone marrow from AML patients in IPO-Porto.

Human plasm, bone marrow fluid and peripheral blood mononuclear cell isolation	
Plasma	BM
1036,4	6053,9
1695,4	8507,2
750	929,6
592,1	1054,6
676,2	962,3
704	1789,8
1415,8	2559,7
1130,7	2489,2
728,7	3844,7
636,1	784,5

- VASCULAR LENGTH AND VASCULAR – N BIOLOGICAL

Table 10 - Means values of vascular length (µm) using a "n" biological for $Nfr2^{flox}$ mice.

MEAN VALUES OF VASCULAR LENGTH (µm) - n biological		
No treatment	**Tamoxifen**	**Tamoxifen + Iron**
1255,042667	848,6823333	1095,595333
1063,502333	742,6363333	1152,0325
1057,824333	1026,280333	1218,815
906,018	829,1073333	1207,535167
698,559	1167,008	1100,270833
	1170,158167	1540,123
	767,1263333	999,1776667
	989,8496667	948,0875

Table 11 - Means values of vascular outgrowth (µm) using a "n" measurement for $Nrf2^{flox}$ mice.

MEAN VALUES OF VASCULAR OUTGROWTH (µm) - n biological		
No treatment	**Tamoxifen**	**Tamoxifen + Iron**
367,6578333	630,7393333	829,629
592,1278333	629,6026667	890,9738333
479,2483333	509,7266667	786,666
654,6613333	664,8366667	663,8795
658,7763333	665,9046667	822,1158333
	738,7356667	878,0266667
	825,003	749,509
	644,859	929,8796667

Table 12 - Vascular length values obtained using a "n" biological for $Nfr2^{flox}$ and $Nrf2^{i\Delta EC/+}$ mice.

Tamoxifen + Iron: Vascular length (µm) – n biological	
$Nfr2^{flox}$	**$Nrf2^{i\Delta EC/+}$**
1095,595333	1303,854667
1152,0325	1024,399167
1218,815	1000,981667
1207,535167	1315,664333
1100,270833	1316,037167
1540,123	1112,762
	1202,101
	939,6526667
	1090,768833
	942,6531667
	922,1203333
	1071,718333
	939,236

Table 13 - Vascular outgrowth values obtained using a "n" biological for $Nfr2^{flox}$ and $Nrf2^{i\Delta EC/+}$ mice.

Tamoxifen + Iron: Vascular outgrowth (µm) – n biological	
$Nfr2^{flox}$	**$Nrf2^{i\Delta EC/+}$**
829,629	785,6165
890,9738333	962,9218333
786,666	884,9306667
663,8795	555,242
822,1158333	689,107
878,0266667	791,8606667
	710,3608333
	818,4033333
	1055,395
	1066,511833
	1070,195
	817,4436667
	818,4863333

- VASCULAR LENGTH AND VASCULAR OUTGROWTH – N MEASUREMENT

Table 14 - Means values of vascular length (µm) using a "n" measurement for $Nfr2^{flox}$ mice.

MEAN VALUES OF VASCULAR LENGTH (µm) - n measurement		
No treatment	**Tamoxifen**	**Tamoxifen + Iron**
1350,886	949,965	1085,163
1355,569	738,097	1210,244
1338,415	857,985	921,06
970,246	859,527	1096,266
1364,736	548,395	1087,678
1150,404	819,987	1173,161
885,63	1135,214	1228,631
1179,524	940,133	808,987
1168,963	1003,494	1161,995
1163,226	927,594	1138,975
975,169	866,197	1410,223
1008,502	693,531	1163,384
866,165	1236,374	1337,668
919,756	1101,491	1146,388

908,528	1163,159	1181,29
1377,284	1148,43	1024,773
1259,111	1225,709	1230,799
1016,102	1175,932	1391,972
879,87	1144,601	1124,339
939,979	1191,274	1212,729
898,205	1135,003	1176,601
745,243	881,552	1201,69
636,691	760,771	1430,539
713,743	659,056	1099,313
	902,688	1465,142
	1050,826	1255,367
	1060,327	757,896
	996,498	880,429
	1018,993	1127,049
	909,766	1115,742
		1619,876
		1297,264
		1703,229
		1030,528
		1088,834
		878,171
		800,325
		1090,109
		908,118
		846,681
		983,43
		1059,862

Table 15 - Means values of vascular outgrowth (μm) using a "n" for $Nfr2^{flox}$ mice.

MEAN VALUES OF VASCULAR OUTGROWTH (μm) – n measurement		
No treatment	**Tamoxifen**	**Tamoxifen + Iron**
420,065	762,41	907,086
211,17	631,292	1013,576
439,906	604,012	987,365
390,77	761,931	923,514
398,77	732,844	621,471
345,266	746,349	701,099
447,138	807,283	672,996
617,862	640,175	813,551
773,918	743,832	496,788
448,705	771,59	903,69
617,796	795,908	523,661

647,348	907,511	753,029
585,976	771,013	631,434
452,63	398,509	674,675
495,041	686,881	757,896
514,65	660,203	624,746
479,705	781,502	814,36
347,488	571,046	963,558
691,944	627,14	977,488
618,663	520,399	794,647
653,377	744,679	944,476
640,888	572,656	986,572
619,885	743,781	703,032
715,556	572,371	698,565
	655,144	828,791
	454,079	721,171
	419,957	1010,504
	636,111	1071,466
	710,715	1055,393
	647,684	689,712
		895,984
		856,219

Table 16 – Vascular length values obtained using a "n" measurement for $Nfr2^{flox}$ and $Nrf2^{i\Delta EC/+}$ mice.

Tamoxifen + Iron : Vascular length (µm) – n measurement	
$Nrf2^{flox}$	**$Nrf2^{i\Delta EC/+}$**
1085,163	1271,775
1210,244	1359,657
921,06	1155,487
1096,266	1505,499
1087,678	1267,435
1173,161	1336,37
1228,631	1126,509
808,987	1238,801
1161,995	972,976
1138,975	1126,509
1410,223	1238,801
1163,384	972,976
1337,668	1137,008
1146,388	1146,944
1181,29	1174,481
1024,773	1208,263
1230,799	1255,889
1391,972	1290,021

1124,339	1308,379
1212,729	1588,052
1176,601	1430,112
1201,69	1097,51
1430,539	1260,234
1099,313	1138,841
1465,142	1088,853
1255,367	949,586
757,896	1122,132
880,429	1033,848
1127,049	969,08
1115,742	982,896
1619,876	887,442
1297,264	1024,232
1703,229	983,596
1030,528	901,015
1088,834	1072,007
878,171	1137,598
800,325	1286,686
1090,109	1499,87
908,118	1160,437
846,681	999,899
983,43	970,98
1059,862	848,079
	979,362
	1166,125
	1041,21
	1079,925
	978,491
	1299,5
	871,251
	919,11
	864,332
	1170,305
	917,384
	913,537
	963,936
	910,009
	892,416
	1107,632
	1186,866
	1022,772
	951,877
	1029,657
	1131,506
	1072,974
	977,483
	768,495
	950,013
	886,552

	979,899

Table 17 - Vascular Outgrowth values obtained using a "n" measurement for $Nfr2^{flox}$ and $Nrf2^{i\Delta EC/+}$ mice.

Tamoxifen + Iron: Vascular outgrowth (µm) – n measurement	
$Nrf2^{flox}$	**$Nrf2^{i\Delta EC/+}$**
698,565	755,462
828,791	668,262
721,171	620,146
1010,504	698,97
1071,466	745,017
1055,393	646,785
689,712	732,694
895,984	909,172
856,219	733,716
662,999	732,694
801,931	909,172
782,11	733,716
808,105	781,737
930,924	749,245
991,705	706,539
881,939	633,896
858,029	473,176
794,887	917,572
890,326	753,129
907,086	881,81
1013,576	933,928
987,365	840,669
923,514	635,882
621,471	668,281
701,099	983,304
672,996	1034,231
813,551	992,243
496,788	922,896
903,69	845,199
523,661	999,658
753,029	899,269
631,434	875,658
674,675	742,14
757,896	1084,707
624,746	875,602
814,36	832,208
963,558	557,956

977,488	409,654
794,647	698,116
944,476	701,572
986,572	876,021
703,032	877,617
	1015,94
	1108,702
	1076,82
	1072,492
	1079,925
	978,491
	946,194
	1001,842
	1103,9
	1083,233
	1026,219
	1237,683
	1077,575
	959,824
	1173,186
	746,735
	871,207
	948,882
	758,48
	885,041
	694,317
	777,117
	904,253
	815,045
	683,025
	914,971
	816,507

- RATIO ASSESSMENT (VASCULAR LENGTH AND VASCULAR OUTGROWTH)

Table 18 – Ratio between Vascular Length and Vascular Outgrowth for $Nfr2^{flox}$ and $Nrf2^{i\Delta EC/+}$ mice.

RATIO (VL/VL+VOg)			
$Nrf2^{flox}$			$Nrf2^{i\Delta/+EC}$
No treatment	**Tamoxifen**	**Tamoxifen + Iron**	**Tamoxifen + Iron**
0,773428409	0,573658175	0,645252593	0,624011801
0,642355011	0,541185853	0,572346267	0,515467389
0,688207107	0,668148214	0,636901438	0,530767867
0,580527967	0,554978857	0,569074115	0,703222983
0,514654694	0,636695911	0,563890812	0,656330447
	0,613003272	0,607741983	0,584242758
	0,481824132	0,571387479	0,628562086
	0,605520535	0,504847751	0,534483922
			0,508241177
			0,469176582
			0,462838547
			0,567298269
			0,534348334

- RATIO N0. ARTERIES AND VESSELS

Table 19 – Ratio of the number of veins and arteries for $Nfr2^{flox}$ and $Nrf2^{i\Delta EC/+}$ mice.

RATIO NO. VEINS AND ARTERIES			
$Nrf2^{flox}$			$Nrf2^{i\Delta/+EC}$
No treatment	**Tamoxifen**	**Tamoxifen + Iron**	**Tamoxifen + Iron**
1	1,25	1	1,2
1	1	1	1,2
1	1,2	1	1
1	1	1	1
1	1,2	1	0,8
1	1	1	0,8
1		1	1,25
1,333333333		0,75	1
		0,6	1
		0,8	1
		0,43	1
		0,43	1
		0,43	1
		1	1
		1	1
		1,25	1
			1
			0,75
			1
			1
			1
			1
			1